DESIGN AND DEVELOPMENT OF AN SSVEP BASED LOW COST, WEARABLE, AND WIRELESS BCI SYSTEM

A THESIS SUBMITTED TO
THE GRADUATE SCHOOL OF ENGINEERING AND SCIENCE
OF BILKENT UNIVERSITY
IN PARTIAL FULFILLMENT OF THE REQUIREMENTS FOR
THE DEGREE OF
MASTER OF SCIENCE
IN
ELECTRICAL AND ELECTRONICS ENGINEERING

By
Abdul Waheed
August 2019

Design and Development of an SSVEP based Low cost, Wearable, and Wireless BCI System
By Abdul Waheed
August 2019

We certify that we have read this thesis and that in our opinion it is fully adequate, in scope and in quality, as a thesis for the degree of Master of Science.

Yusuf Ziya Ider(Advisor)

Behçet Murat Eyüboğlu

Hacı Hulusi Kafalıgönül

Approved for the Graduate School of Engineering and Science:

Ezhan Karaşan
Director of the Graduate School

ABSTRACT

DESIGN AND DEVELOPMENT OF AN SSVEP BASED LOW COST, WEARABLE, AND WIRELESS BCI SYSTEM

Abdul Waheed
M.S. in Electrical and Electronics Engineering
Advisor: Yusuf Ziya Ider
August 2019

It has become a challenging research topic to design and develop cheap and wearable brain-computer interface (BCI) systems but not compromising the performance. In this thesis, the design and development of a steady state visually evoked potential (SSVEP) based BCI system has been presented which is a low cost, wearable BCI system and gives highly accurate target identifications with good information transfer rate (ITR). It is a battery powered, wireless BCI system and ensures the complete isolation to the subject. Like all the BCI systems, it is designed and implemented in five major parts: (i) stimulator which is a microcontroller based circuit and provides the frequency modulated visually evoked potential (f-VEP) and code-modulated visually evoked potential (c-VEP) stimulations (ii) dry active electrodes which capture the electroencephalography(EEG) signals from the O1, O2, and Oz head positions (iii) high sampling rate, 4-channel EEG data acquisition hardware which acquires the EEG signals, amplify them, converts them to digital data, and transmits the data using wifi communication (iv) the data processing unit (DPU) which is a MATLAB script to process the raw EEG data and displays the results and (v) the headset which mounts all the components except DPU and is developed using 3D printing technology. The first prototype of the proposed BCI system has been developed in 331 USD and tested for both the f-VEP and c-VEP modalities on six human subjects. For f-VEP modality, it exhibits an average accuracy (live accuracy) of 92.1% and average ITR (live ITR) of 69.5 bits/min on the basis of target identifications done on 1.04 s data recordings. If we extract one message character from five consecutive target identifications, the average message accuracy goes to 98.8% and average message ITR to 17.2 bits/min. In case of c-VEP modality, it exhibits live accuracy of 70.1 % and live ITR of 23.5 bits/min while message accuracy of 90.7 % and message ITR of 12.4 bit/min.

Keywords: BCI system, SSVEP, low cost, wearable, wireless.

ÖZET

DHGUP BAZLI UCUZ VE GİYİLEBİLİR BİR TELSİZ BBA SİSTEMİNİN TASARIM VE GELİŞTİRİLMESİ

Abdul Waheed
Elektrik ve Elektronik Mühendisliği, Yüksek Lisans
Tez Danışmanı: Yusuf Ziya Ider
Ağustos 2019

Performanstan ödün vermeden ucuz ve giyilebilir bir beyin-bilgisayar arayüzü (BBA) sisteminin tasarımı ve geliştirilmesi zorlayıcı bir araştırma konusu olmuştur. Bu tezde, ucuz ve giyilebilir olan, büyük oranda hatasız hedef belirlemesi yapabilen, ve kabul edilebilir Enformasyon Transfer Hızına (ETH) sahip olan, Durağan Hal Görsel Uyarılmış Potansiyel (DHGUP) bazlı bir BBA sisteminin tasarım ve uygulaması sunulmaktadır. Bu system bataryadan beslemeli ve telsiz olduğundan özneye tam izolasyon sağlamaktadır. Tüm BBA sistemleri gibi 5 kısım olarak tasarlanmış ve uygulanmıştır: (i) Frekans Modülasyonlu Görsel Uyarılmış Potansiyel (FMGUP) ve Kod Modülasyonlu Görsel Uyarılmış Potansiyel (KMGUP) uyartımlarını sağlayan mikrokontrolör bazlı uyarıcı, (ii) Elektroansefalogram (EEG) sinyallerini O1, O2, ve Oz kafa pozisyonlarından kaydetmeye yarayan kuru aktif elektrotlar, (iii) EEG sinyallerini yükselten, sayısala çeviren ve telsiz haberleşmeye gönderen 4-kanallı yüksek örnekleme hızlı veri toplama sistemi, (iv) Bilgisayar/laptop tarafında Matlab kullanan, ham veriyi işleyen ve sonuçları gösteren Veri İşleme Ünitesi (VİÜ), (v) VİÜ dışında tüm bileşenleri taşıyan ve 3D yazıcı teknolojisiyle ile geliştirilmiş olan kafalık. Önerilen sistemin ilk prototipi 331 ABD doları altında bir komponent maliyetiyle üretilmiş ve 6 denekde FMGUP ve KMGUP modalitelerinin her ikisi için de denenmiştir. FMGUP modalitesinde, 1.04 saniyelik kayıtlardan anında yapılan hedef tespitlerinde, ortalama "canlı doğruluk" yüzde 92,1 ve ortalama "canlı ETH (Enformasyon Transfer Hızı)" 65.5 bit/dakika olmuştur. Peşpeşe 5 hedef tespiti sonucunda bir mesaj çıkarma yapıldığında ortalama "mesaj doğruluğu" yüzde 98.8 ve ortalama "mesaj ETH" değeri 17.2 bit/dakika olarak ölçülmüştür. KMGUP modalitesinde ise "canlı doğruluk" yüzde 70.1 ve "canlı ETH" 23.5 bit/dakika olurken, "mesaj doğruluğu" yüzde 90.7 ve "mesaj ETH" değeri 12.4 bit/dakika olmuştur.

Anahtar sözcükler: BBA sistem, DHGUP, ucuz, giyilebilir, telsiz.

Acknowledgement

First of all thanks to Allah with whose mercy I am going to complete Masters degree in the challenging field of electrical engineering. At this big moment, how can I forget my parents who always keep praying for me. I always have a safety cover of their love hearted prayers due to which I feel much smoothness in the proceeding of my life. I am much thankful to my wife (Humaira) who always stand by me in every thick and thin of my life. She kept pushing me until I made my mind to do masters after a long gap of 7 years from completing my BS engineering. I also want to take the opportunity of this big moment to thank my uncle (mamu Abdul Wahid) and aunt (phupho Sharifan) for their always kind behavior and sincere prayers. I also want to thank all my family members for always giving me respect and love.

I highly acknowledge the biggest contribution of my advisor "Prof Yusuf Ziya Ider" who remained kind to me and guided me to fulfill my degree requirements. He talked to me not only on the technical topics but also on many other socio-political topics. I always enjoyed to have conversations with him. I also want to pay my best regards and bundle of thanks to Suleman memon who always helped me in technical difficulties as if they were his problems. I am also thankful to Muhammad Nabi, Toygun, Yiğit, and çelik who made the working environment friendly and peaceful.

I want to thank Türkiye Bilimsel ve Teknolojik Araştırma Kurumu (TÜBİTAK) for supporting this study through research grant 114E153.

I could not be able to start masters degree without the motivations given by my beloved boss at my office "Dr. Shahid Ali". He encouraged me to excel in my studies and spared me from office duties for this purpose. I cannot forget the motivational lectures of Kashif Iqbal. The kindness of Inam Bhai is also a great factor to persue my degree. I would like to thank all of my office colligues and friends like Sajjad Usmani, Nisar, Yasir, Shoaib, A.Wahid, Asif, Rafaqat, Faisal, Usama, Shamoon, Sufyan, Saad and many more. My love goes to Raghib, Raziq,

Zeeshan, Amjad, Arshad Shakir, Sajidullah and Mazhar.

Life becomes boring without friends. I also want to thank all my friends who help me to live far away from home country in a lively and joyous way. I have spent one of my best spans of life in Bilkent University which is memorable due to my minions group (Bareera Bhabi, Naveed, Talha, Furqan, Zakwan and Saeed Ahmed). I want to say special thanks to Zakwan and Saeed to keep me with them at all hangouts. It was an unforgettable time spent with them. I can never forget the ever smiling face of Anjum Bhai and Faiza Bhabi and their always helping nature. I also want to thank Zakaullah, uncle GM, Abdul Hakeem, Abdul Wahid and Sajid Amin to remain in contact and supportive to me during my stay at Bilkent.

I am also thankful to my brother Waqar Ahmed who took my charge of fulfilling the domestic responsibilities and took a very good care of my children in my absence. I also want to take the opportunity to thank my cousin and best friend Imran with whom I can share everything.

At this moment, I want to remember my grandmother with whom I spent best days of life (Childhood). May Allah rest her soul in peace and reward her a high place in paradise. As last words, **I want to dedicate this thesis to my parents, to my wife, and to my children (Abdul Aleem, Abdul Ahad, and Manha Abdul Waheed)**.

Contents

List of Figures

List of Tables

Chapter 1

Introduction and Background

1.1 Background

1.1.1 Brain Computer Interface (BCI)

As the name suggests, the brain-computer interface(BCI) systems provide a direct link of communication between the brain and the external world (e.g. computer or any other electronics device). They do not need any physical device or typical muscular activity for delivery of information to the outside world. Normally if we want to give some command to a simple coffee making machine, the brain initiates cognitive processes and then activates particular motor activity and our hand presses the button to complete the interaction with the machine. In case of BCI systems all these intermediate activities are bypassed and the signal from brain is directly interpreted to start the device accordingly. In other words, BCI systems form a communication bridge between the brain and the outside physical world. They manage to send messages directly captured from the brain of handicapped people to the computer or some other device to help them to communicate their silent ideas or opinions using variety of BCI application like BCI speller application[1], semantic categorization[2], or silent speech communication[3].

The motivation behind the development of BCI systems is the fact that certain features of the brain activity signals are linked to the specific mental states. Therefor, a BCI system measures one or more of these features and translate them to certain meaningful commands to interact with the devices/machines. The features which have been used in the previous studies include neuron's actions potentials (APs) recorded from the cortex, event related potentials (ERPs) recorded from the cortex[4] electroencephalography (EEG) features like p300 evoke potential, visually evoked potential (VEP), magnetoencephalography(MEG), functional magnetic resonance imaging(fMRI), and positron emission tomography (PET) [5]. The recordings of APs and ERPs from cortex, head surgery is required which may cause medical complications while MEG, fMRI and PET are technically complex and much expensive techniques. Since EEG technique is fast, cheap and easy to implement, it is widely used in the modern research of BCI systems.

A typical BCI system involves several generic steps to establish a direct interactive link between the brain and the external device/machine, as follows [6]:

a. **Signal acquisition:** Acquisition of the brain signals (includes electrodes to capture the brain signals, buffering and amplification, analog to digital (A/D) conversion and communication to the computer etc.)

b. **Preprocessing:** Converting raw data for further advanced steps

c. **Feature extraction:** Extraction of desired features from the data

d. **Classification:** Classification on the basis of the extracted features

e. **Translation:** Converting classified feature into computer command

f. **Application Interface:** The interface between computer's commands and the real application

figure 1.1 describes all the above steps graphically.

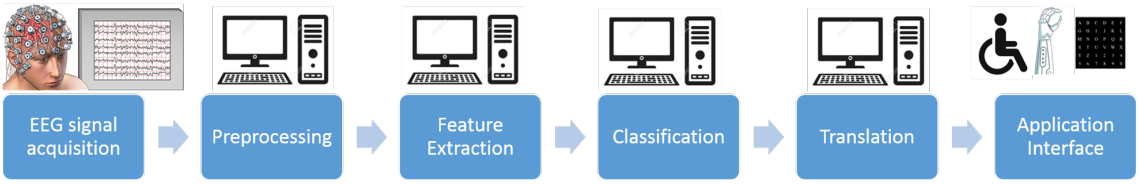

Figure 1.1: General Structure of a BCI system

On the basis of the technique used from data acquisition, the BCI systems can be categorized in three groups as follows:

1.1.1.1 Invasive BCI Systems

These BCI systems acquire brain signals directly from the cortex, so to implement such systems scalp surgery is required to implant the electrodes into gray matter. The main advantage of using invasive techniques is to get better signal quality and more accuracy as the signals are directly acquired from the brain without even having the scalp in between[6]. But this may lead severe medical complications as the body of the patient may not accept the implanted electrodes. The scar tissues may be formed as a reaction to the surgery, which will cause to weaken the brain signals [6][7]. The research on invasive BCI systems is mainly focused on the repairing of damaged visual system and provide some movement options to the paralyzed people.

1.1.1.2 Partially Invasive BCI Systems

In partially invasive BCI systems, the electrodes are implanted subdurally on the brain's surface inside the skull but the system rests outside the brain (i.e., the electrodes do not penetrate to the gray matter). An example of such systems is electrocorticography (ECoG). The partially invasive BCI systems enjoy the advantages of very high signal quality, lesser susceptibility to various artifacts than non-invasive techniques, high spatial resolution ($< 1cm$) and high temporal resolution ($< 1ms$) [6]. The disadvantage of the partially invasive techniques is again

the risk of a permanent hole in the skull which may cause medical complications [6].

1.1.1.3 Non-invasive BCI Systems

The non-invasive BCI systems installed outside the brain and the signals are acquired from over the skull. In this technique, the signal quality becomes very poor because much of the signal's power gets damped by the scalp. Also there is dispersion and scattering of the electromagnetic waves generated by the neurons [6]. Although the quality of the signals is low in this technique, substantial majority of the research in the field of BCIs has used non-invasive EEG based BCI systems. The reason behind this is obviously its easy implementation without having risk of medical complications.

1.1.2 Electroencephalography (EEG)

EEG provides the measure of the electrical activity taking place in the brain as a result of synaptic excitations of the neurons [8]. It can be classified into five sets of signals based on their frequency ranges. These sets are named as delta (δ), theta (θ), alpha (α), beta (β) and gamma (γ) signal [8]. The band of delta(δ) signal lies below 4 Hz and it is more prominent in babies and its amplitude decreases with the age. In adults, it is detectable only in deep sleep state [8]. $4-7$ Hz band is named as theta (θ) waves. In a normal adult in awake state, the EEG activity in the theta (θ) band is very small while it is larger in children, and adults in drowsy, sleep and meditative states [9]. Alpha(α) waves lie in $8-12$ Hz range and they are found over the occipital lobe of the brain [10]. The amplitude of these waves become prominent when eyes are closed and the body is relaxed. It starts disappearing as the eyes are opened and mental activity comes into play. So the alpha waves can be associated with the mental effort [11]. Beta (β) waves lie in the range of $12-30$ Hz. They are associated with motor activities taking place in the brain's central and frontal regions. They are symmetrically distributed when

there is no motor activity but as soon as there comes some active movement, its distribution becomes unsymmetrical and amplitude is attenuated [12]. The band ranging from $30 - 100\ Hz$ is termed as gamma (γ) waves. In a healthy human, these waves are associated to certain motor functions [13] like maximal muscle contraction [14]. Gamma waves are not commonly used in the EEG based BCI systems because they are easily affected by the artifacts like electromyography (EMG) or electrooculography (EOG) [15].

EEG signals can be captured easily from the scalp surface and there is no need to make a hole in the scalp to capture the signals. This feature of the EEG signals makes it a most popular technique among the people doing research in the field of BCI [8]. However, there is a big challenge ahead to use these signals for the purpose of building the BCI systems. The problem is that the EEG signal's quality recorded from the scalp is very poor because the signal has to face attenuation, scattering and blurring effects [6] while crossing the skull, scalp and many other layers [8]. This means that the acquisition of reliable EEG signals from the scalp is not that easy. Moreover, the EEG signal (having amplitude of the order of μV) is very prone to be affected from the various noise sources inside and outside the brain [8]. External sources include power line which may generate 50/60 Hz background noise and internal sources cause thermal, flicker, burst and shot noises [16]. So, the EEG signal acquisition stage should contain such a good quality EEG signal acquisition system (electrodes, amplifiers, A/D converters) which not only record the signal but also prevent it from getting affected by the surrounding noises.

The EEG signal is acquired by measuring the potential difference between the desired electrode position (active position) and the reference electrode position (reference position). A third electrode position (known as ground position) connected directly to the electronic circuit's common is also used for the acquisition of differential voltage signal between the active position and the reference position. So minimum of the three electrodes are required to acquire the EEG signal from some position over the head. The physical positions of the electrodes over the scalp were first described by developing the 10-20 international system [17] to acquire repeatable results from multiple recordings. The 10-20 international

system standardizes the placement positions of the EEG electrodes on the basis of external landmarks and regular separation between the electrodes [18]. It uses two points of the head as reference to define the electrode positions. One of these two reference points is named as "Nasion" while the other as "Inion". The Nasion is marked on the top of the nose at the level of the eyes while the Inion is present at the bony lump at he skull's base. The 10-20 international system diagram is shown in Figure 1.2:

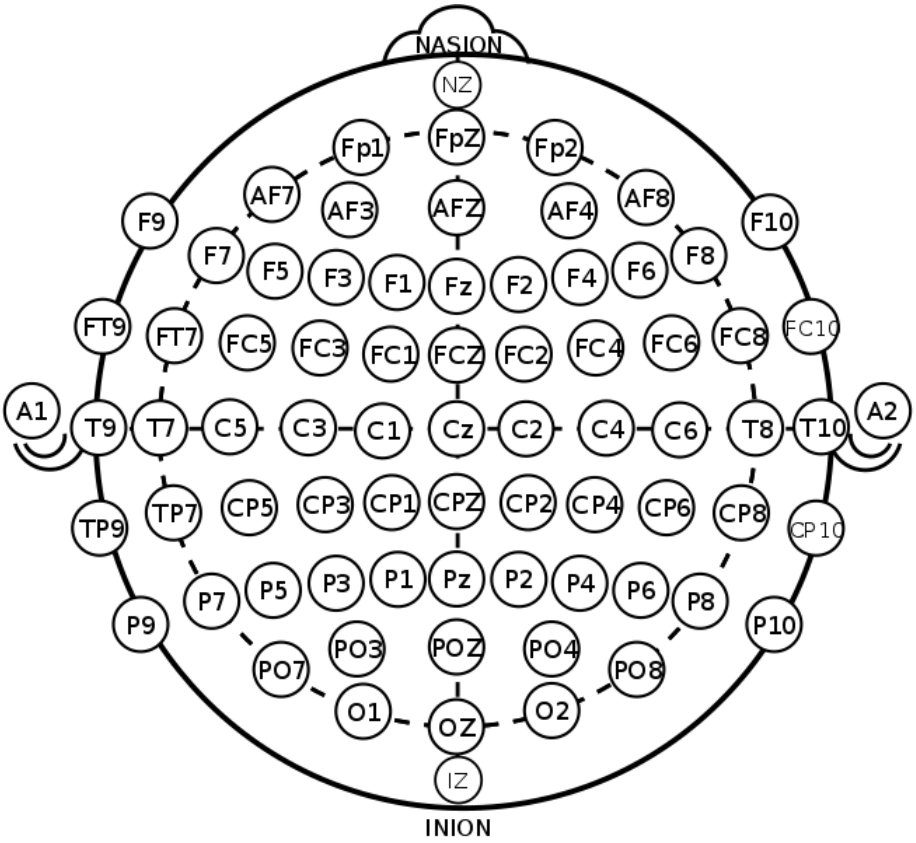

Figure 1.2: Electrode positions over the skull described by 10-20 international system

In the above figure, letter symbols are used to represent the specific regions of the brain. Letter C corresponds to the central region, P to the parietal lobe, F to the frontal lobe and O to the occipital area. The regions between these areas are represented by combination of these letters such as CP represents the region between central and parietal area.

1.1.3 EEG Based BCI Systems

EEG based BCIs are widely employed by the researchers due to minimum health risks and it is relatively convenient to conduct studies and to find volunteer human subjects [19]. Since BCI systems are supposed to provide a link between the recorded brain activity and the user's intentions, there should be some correlation/linkage among the user's wills/actions and the brain activity. The EEG signals consist of a very large number of simultaneous phenomena taking place due to cognitive tasks. Out of such a large number of simultaneous responses researchers should be able to decode a few physiological phenomena so that they can be modulated with the user's intentions. The most commonly used modalities in the current BCI systems are P300 evoked potentials, sensorimotor rhythms (SMR), slow cortical potentials (SCP), and visually evoked potentials (VEP) [8].

1.1.3.1 P300 Evoked Potential

The first BCI system based on P300 evoked potential was reported by Farwell and Donchin[20] in 1988. The control signal in this BCI system was a positive potential which appears after 300 ms from the occurrence of target stimulus. The P300 signal can be extracted from the EEG recordings by simply averaging it [19]. In P300 evoked potential modality, the stimulus is designed such that there are some frequent events called non-target stimuli and one is the rare event termed as target stimulus. These events may be related to the visual, auditory or somatosensory stimuli [8].

Farwell and Donchin presented to their subjects a 6×6 matrix containing alphabets (A-Z) and some symbols. The rows and columns of the matrix were intensified in a random way and the subjects were asked to focus on the target letter/symbol and perform some mental task (e.g., counting in mind the number of times the target letter/symbol is flashed). In this way they implemented a speller BCI using P300 evoked potential. An example of the 6×6 matrix which can be used as stimulator in P300 speller BCI is shown in Figure 1.3.

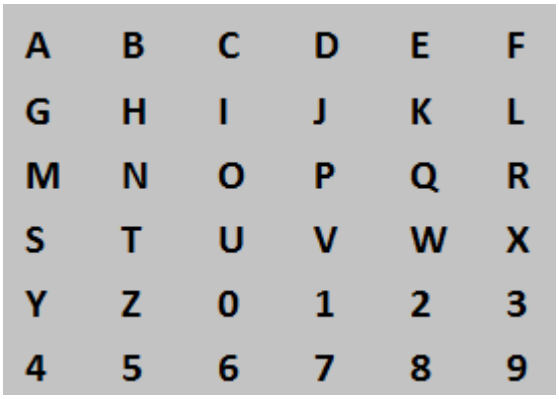

Figure 1.3: A 6×6 matrix of alphabets and numbers which can be used for BCI speller application

Since P300 signal is obtained by averaging the EEG signals, numerous trials of the experiment are required to get the p300 evoked potential signal. So, the information transmission rate (ITR) and accuracy of the P300 based systems are low [21]. Many studies are held to improve both of these parameters. Accuracy can be improved by designing a complicated classifier instead of using simple average [21][22]. The detection accuracy of P300 based BCI employing visual stimuli is also dependent on the size and color of the letters/symbols. The small sized letters/symbols give low detection accuracy [23]. The green blue chromatic flicker gives more accuracy while gray black chromatic flicker gives less accuracy [24][25]. ITR can be improved by employing modern techniques of error detection and correction in the real time [26].

1.1.3.2 Sensorymotor Rhythms (SMR)

When a person thinks or performs some movement related tasks, the changes in the amplitudes of the signals lying in alpha and beta frequency bands have been observed [27]. Many studies in this field have revealed that the movement imagination (known as motor imagery) may amplify or suppress the EEG amplitudes from the sensorimotor areas of the brain [27][28]. On the basis of these two amplitude modulation behaviors, the SMRs can be divided into two categories named

as ERD (event-related desynchronization) and ERS (event-related Synchronization) [12]. ERD corresponds to the suppression of the EEG amplitudes while ERS to its enhancement as a result of motor imagery or actual motor activity.

Apart from the changes in amplitudes of alpha and beta band's signals, the amplitude variation is also observed in the gamma band (relatively higher frequencies) and very low frequency band ($< 1\ Hz$) [28][29]. In short, SMR contains considerable amount of complementary kinematic information about the motor activity and motor imagery. This very important neurophysiological information has been decoded and made part of the many BCI controls [29]. The well known examples of such BCI systems utilizing SMRs are Graz [30], Berlin [31] and Wadsworth [32] BCIs.

1.1.3.3 Slow Cortical Potential (SCP)

As the name suggests, SCPs are the slow changes in EEG amplitudes. The changes can take one or more than one second to occur. So, this activity exhibits less than 1 Hz frequency band of the EEG signal [33]. The SCP level is inversely related to the neuronal activity in the cortex i.e. increased neuronal activity in the cortex gives rise to the negative SCP while the decreased neuronal activity to the positive SCP [33]. These SCP shifts can be employed to develop BCIs for cursor control or target selection on the screene [34]. In these BCIs the human subjects were trained to trigger these SCP changes by using the thought-translation device [34]. Thought-translation device helps the users to learn how to correlate their thoughts with the SCP changes using some visual auditory marks. The success of the SCP self regulation training is dependent on various factors such as subject's mental and physical states, social context and motivation [34].

Accordingly, the performance of SCP based BCIs is much dependent on the quality of the SCP self regulation training which also varies with person to person. The performance also depends on the mood, pain and sleep quality of the user [34]. The accuracy achieved by employing the SCP classification modality lies between 70% and 80% and the ITRs achieved are relatively low [8]. Also the

training process of the SCP based BCIs is very slow. It can take several months to train the self regulation SCPs with the user [8].

1.1.3.4 Visually Evoked Potential (VEP)

VEP is the EEG brain activity taking place in the visual cortex of the brain as a result of presenting some sort of visual stimulus to the subject [35]. The amplitude of the VEP substantially increases as the visual stimulus enters the central visual field [36]. Thus it becomes very easy to use this modality in the BCI systems. There are three different criteria to classify the VEPs [37]:

a. **On the basis of optical morphology of the stimulus:** VEPs can be observed as flash stimulations or graphical pattern stimulations such as random dot map and checkerboard lattice [8]

b. **On the basis of the field stimulation:** This criteria divides the VEP modality into three categories termed as whole field VEP, partial field VEP and half field VEP. For example, half of the monitor screen is used as the visual stimulus while the other half has no stimulation and the subject is focusing at the screen's center during the experiment, then the resulting VEP response is called half field VEP [8].

c. **On the basis of frequency of the visual stimulus:** The frequency of the visual stimulus divides the VEP modality into two major categories known as transient visual evoked potential (TVEP) and steady state visually evoked potential (SSVEP). TVEPs can be observed for the stimulation frequencies below $6Hz$ while the SSVEPs require relatively higher frequency of stimulation [35][38]. TVEPs can be observed by making any change in the visual field. The most commonly used TVEPs include flash TVEPs, pattern onset TVEPs, pattern offset TVEPs, and pattern reversal TVEPs [39]. The TVEP responses differ with the nature of the stimulus. The flash TVEPs exhibit two prominent voltage peaks $N2$ (negative) and $P2$ (positive) at $90ms$ and $120ms$ respectively from the onset of the flash, pattern

TVEP exhibit $C1$ (positive), $C2$ (negative) ,and $C3$ (Positive) peaks at $75ms$, $125ms$, and $150ms$ respectively, and pattern reversal TVEP exhibits one negative, one positive, and one negative peak at about $75ms$, $100ms$, and $135ms$ respectively [39]. The SSVEPs can be provoked in the visual cortex by presenting the light source flashing at some frequency greater than $6Hz$ or having some code or time based modulation. In case of flashing stimulus, the SSVEP response is the sinusoidal wave having fundamental frequency equal to the flashing frequency [8].

In a typical VEP based BCI system, SSVEP is the commonly used modality because it is less susceptible to the noise/artifacts caused by eye movements [40], eye blinks [40], and EMG [41] than the TVEPs. Also in contrary to the TVEPs, the amplitudes and phases of the relative frequency components in SSVEP show much less variability over longer periods of time [42].

1.1.4 SSVEP Based BCI Systems

In SSVEP based BCI systems, the target is detected upon fixing the subject's eye gaze. This procedure needs user's full attention. The target is normally a light source which can be driven by a stimulus sequence signal modulated differently. The SSVEP based BCIs may have numerous flashing light sources driven by different stimulus sequences/signals. The VEP response generated in the visual cortex as a result of presenting these multiple stimuli sequences to the user should be nearly orthogonal to each other in some domain to ensure reliable target identification [43]. On the basis of the modulation type of the stimulus signal, the SSVEP based BCI systems can be divided into three main categories [43]:

a. **Time modulated VEPs (t-VEPs):** In this case, the targets are flickered by the signals which are orthogonal to each other in the time domain. It means that the flashing signals driving the light source should be strictly uncorrelated/non-overlapping in the time domain [8]. t-VEPs based BCIs

need no training sessions prior to the experiment but they exhibit very low ITR ($< 30 bits/min$) and they are not so simple to implement as they need proper synchronization of the stimulus signals [8].

b. **Frequency modulated VEPs (f-VEPs):** In case of f-VEPs the light sources are driven by the signals (sinusoidal or square waves) having unique frequencies. The VEP brain responses to these flashes (EEG signals) contain the fundamental as well as harmonics of the target frequency [8]. The BCI systems employing f-VEPs are the simplest ones as they don't need any synchronization among the flashing signals and also don't need any training sessions but the number of targets cannot cross the limit of a few. They also exhibits high ITR values typically in the range of $30 - 60 bits/min$ [8]

c. **Pseudo-random code modulated VEPs (c-VEPs):** In case of a c-VEP based BCI, the flash signal is a code whose HIGH and LOW states are determined by a pseudo-random sequence. These systems are much suitable when the number of targets are many and also they exhibit very high ITR values ($> 100 bits/min$) [8]. The implementation of these systems is relatively harder as they need proper synchronization among the stimuli and the training sessions prior to online/real-time tests.

The typical technique used for the stimulation in SSVEP based BCIs is flashing the light sources. For instance, alphabets, digits or symbols flickering on the screen and the subject focuses his/her gaze on one of them or changes his gaze to give some message to the computer [44]. For this purpose, the user has to concentrate on the flashing screen points for some time duration which may not be suitable for the ALS (Amyotrophic Lateral Sclerosis) patients at the advanced stages, or the patients having disability to control their neck or eye movements [8].

Since the stimuli for typical SSVEP based BCIs are flickering light sources, three main hardwares are commonly used: cathode ray tube (CRT) monitors, light emitting diodes (LEDs) and liquid crystal displays (LCDs) [8]. The implementation of the SSVEP stimulator on the LCD and CRT monitors is relatively

easier as they can be easily connected with the computer while the LEDs need specific hardware to generate visual stimuli. The number of targets on the LCD and CRT monitors are also limited by their refresh rates while the LED based stimulator may have numerous targets because the LEDs are independently driven by a logic device like FPGA [45]. Hence, the stimulator type can be decided on the basis of the number of targets/options [46]. LCD screen is the optimal choice for the BCIs having less complexity (< 10 options) because it causes less fatigue to the eyes than in case of CRT monitors. In case of medium complexity (i.e., BCIs having $10 - 20$ options) both the CRT or LCD screens are the optimal options. LED based stimulator designs are optimum choice for the BCIs having more than 20 options.

Since SSVEP based BCI systems provide a large group of discrete control commands and a high reliability, they have attracted many BCI researchers [47]. A lot of BCI applications have been developed using SSVEP paradigm such as high speed spellers to write the text [48][49], control of humanoid robot [50], control of lower limb exoskeleton [51], electrical prosthesis [52] and an orthosis [53] and navigation control in 2D BCI games [54].

1.1.5 Practical BCI Systems

The BCI systems provide alternative means of communication and control between the brain and the real environment. Thanks to the BCI researchers who have used new and modern techniques in the relevant fields (e.g., data acquisition and signal processing) and have made the BCI systems more practical and reliable. These advancements in the BCI technology are mainly targeting the people with severe motor disabilities (patients with locked-in states) [8]. In recent research, many BCI applications have been devised to make the life of the locked-in patients easy and independent from the caretaker services [8]. Some of the major fields of implementation of the BCI systems are described briefly as follows:

a. **Communication:** These BCI applications provide the users a way to express their thoughts hidden due to their disability to speak. Such application usually include BCI spellers which aid the users to write text by presenting them the matrix of alphabets, numbers and certain symbols. A lot of research effort has been put to implement and enhance the performance of the BCI spellers (e.g., [55] and [56] used P300 evoked potentials, [57] used SSVEP, [58] used c-VEP, and [59] used hybrid paradigms).

b. **Motor Restoration:** The patients suffering from spinal cord injury sometimes lose their movement abilities. BCI application can be developed to restore some of the motor actions. For instance, in [60], BCI application was developed to make a tetraplegic patient able to hold a cylinder by his paralyzed hand.

c. **Environmental control:** The BCI applications related to environmental control mainly target the homebound patients to communicate with their surrounding environment like home appliances control [8]. For instance, A prototype design of BCI system integrating with the home environment is presented in [61].

d. **Medical applications:** BCI systems can be proved instrumental by providing neurofeedback to influence the brain for some behavioral changes [8]. Such BCI systems can be used to improve the patient's cognitive performance [62][63], affection [64], speech skills [65] and pain management [66]. These BCI systems may also be used to cure some of the mental disorders like attention deficit [67], epilepsy [68][69], depression [70], schizophrenia [71], paedophilia [72], and alcohol dependence [73] etc.

e. **Locomotive control:** BCI research is also focusing on making the disabled people able to drive some means of transportation like wheelchair etc. to make them more autonomous and independent [8]. In [74] and [75], some experiments were performed to study the feasibility of the use of BCI systems to continuously control the mobile robot in an indoor domestic environment containing rooms, doors and corridors etc. These studies made the researchers focus on developing EEG based portable BCI systems

for continuous wheelchair control for the disabled persons. The research presented in [76] and [77] discuss such EEG based BCI systems.

1.2 Objective and Scope

In recent research on SSVEP based BCI systems, people are found to focus on designing the algorithms for obtaining high ITR [78], developing applications for real time control of systems like drones [79] etc., finding strategies for the users to perform cognitive activity during BCI experiments [80], and performing spatial analysis techniques to make signal quality better [81]. In all these studies, multichannel data acquisition is required. Since wearability of the BCI system is increased by reducing the number of EEG recording channels, it becomes a challenging research topic to design and develop such BCI systems which are not only wearable but also give good performance and are low in cost [82].

In this thesis the design and development of an SSVEP based low cost, wearable, and wireless BCI system is presented. The use of open source and off the shelf components makes it easier to achieve its low cost feature. It provides three channel, differential EEG acquisition at high sampling rates (up to 2000 samples/s) from dry active electrodes placed at O1, O2, Oz and FCz positions. It is capable of detecting the user's gaze in real time when he/she focuses his/her gaze at one of the three LEDs for at least three seconds. It is a generic SSVEP based BCI system which can either be used to implement f-VEP or c-VEP modality to distinguish among the targets. With the implementation of f-VEP modality, the system gets an added advantage of being trainingless. In other words, it does not need any training prior to start of the experiment on the subject.

This proposed BCI system can be used to develop many real time applications for the patients with motor disabilities to interact with their surroundings such as control of wheelchair, humanoid robot and home appliances. Since such patients become home bound, these applications enable them to improve their life standard by making them independent from their caretakers. These applications also

provide relief to the relatives of the patients because they do not need intensive care in the presence of these aids.

1.3 Organization of the Thesis

This thesis consists of total five chapters. The first chapter includes the background, introduction and objective of the thesis. The design and development of all the individual parts of the proposed BCI system is discussed in detail in chapter 2. The experimental procedures to evaluate the performance of the system are described in chapter 3 and the results along with discussion are presented in chapter 4. The conclusion is provided in chapter 5.

Chapter 2

Design and Implementation of the Proposed BCI System

The proposed BCI system is divided into five main parts as listed below:

a. Stimulator

b. Dry active electrodes

c. EEG data acquisition hardware

d. Data processing unit (DPU)

e. 3D printed headset

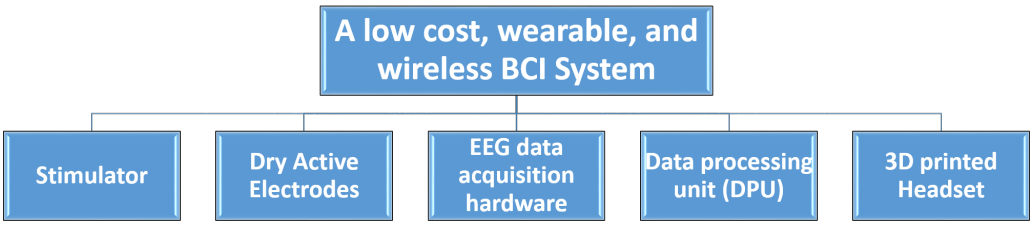

Figure 2.1: The Breakdown structure of the proposed BCI system

Before going into the design and implementation of the parts mentioned in Figure 2.1, a brief overview of the system functionality is presented. The proposed BCI system uses three LEDs (named as Left (L), Center (C) and Right (R) w.r.t the subject) as visual stimuli. Each LED flickers at one of the three different frequencies in case of f-VEP experiment or according to the pseudo-random code sequence in case of c-VEP experiment. The differential EEG data is recorded using dry active electrodes from O1, O2, and Oz positions with respect to the reference position FCz. The data acquisition is done using a 4-channel EEG data acquisition hardware. Fourth channel is dedicated for the marker signal in case of c-VEP experiments. The acquired EEG data is then processed in real time to estimate the subject's focus. In simple words, the subject is asked to focus at one of the LEDs and our system estimates his/her focus (L, C or R) in real time. This complete flow of information is described in Figure 2.2. The detailed design and implementation is discussed in the upcoming sections.

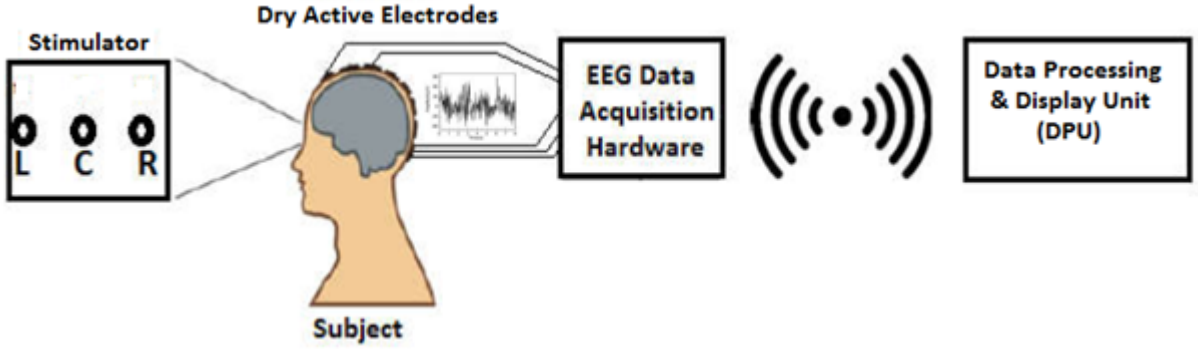

Figure 2.2: Flow diagram showing the flow of data through the system

2.1 Stimulator

The purpose of the stimulator is to provide the visual stimulus to the brain, in response of which brain generates specific signals used to classify the targets. Since the proposed BCI system is based on steady state visually evoked potentials (SSVEP), the stimulator is designed in such a way to provide both the frequency modulated VEP (f-VEP) and code modulated VEP (c-VEP) stimulations according to the requirement of the experiment.

The proposed stimulator design consists of three LEDs driven by a battery powered, microcontroller based circuit. So the whole stimulator design can be disintegrated into three parts (battery, LEDs, and stimulator circuit) as described in the upcoming paragraphs:

2.1.1 Battery

To power up the whole stimulator, a 7.4V, Lithium-Polymer (LiPo) rechargeable battery is used. It is a Lithium-ion rechargeable battery using the polymer as electrolyte instead of liquid. The representative image of the battery is shown in Figure 2.3

Figure 2.3: The $7.4V$ Lithium polymer rechargeable battery

The battery has following key features:

a. It contains two battery cells placed in series having nominal voltage of $3.7\ V$ each making the total nominal voltage of $7.4\ V$.

b. Its rated capacity is $2400\ mAh$.

c. Discharge cut-off voltage = $6.0\ V$. It means that it can be used for the output voltage as low as $6.0\ V$. If the current is drawn after reaching this low threshold, the battery may become inactive and will not be able to recharge.

d. It can be charged by the DC supply of 8.4 V and $0.5 \times C = 1.2$ A where C is the rated capacity of the battery.

e. It can be discharged at $0.2 \times C = 0.48$ A until the voltage drops to 6.0 V.

f. It is 80.5 mm in length, 50.5 mm in width and 12 mm in thickness.

2.1.2 Light Emitting Diodes (LEDs)

Three in number 3W power LEDs, emitting white light are used as the stimulation source. They are cheap and easily available from the local market. The representative image of the LEDs is shown in figure 2.4

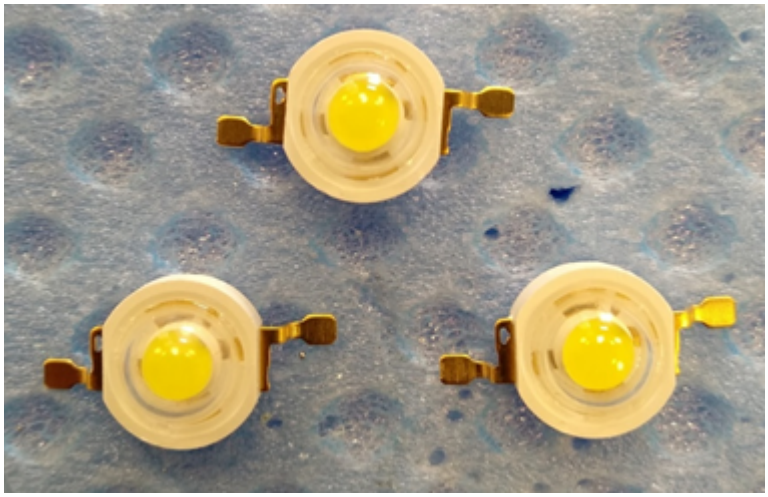

Figure 2.4: The representative image of the Power LEDs used in the stimulator

Some of the key features of the LEDs are described below:

a. Light color = white

b. Forward voltage drop = 3.0 V to 3.2 V

c. Viewing angle = $125 \pm 5°$

d. Luminous flux = $160 - 240$ Lumens.

e. Bulb diameter = 6 mm

f. Mounting type: Surface mount with 5 mm total height

The LED array was formed to place the LED targets as close to each other as possible so that gaze shifting would require minimal eye movement. For less than 5 cm separation between the LEDs, it becomes difficult for the user to focus on certain LED target because the neighbouring LED generates the flickering perception different from that of target LED in the user's mind. For the separations greater than 5 cm, the results were neither deteriorated nor improved. So, a separation of 5 cm between the consecutive LEDs is used.

Similarly for the distance of LEDs less than 15 cm from the forehead, the user feels it difficult to focusing the target LED. For more than 15 cm distance of LEDs from the forehead, the results did not change. So, The three LEDs are arranged in the form of a horizontal array formed in such a way that they are 5 cm apart from each other keeping the distance of the whole array from the subject's forehead as 15 cm. The LEDs array mounted on the 3D printed headset is shown in figure 2.5.

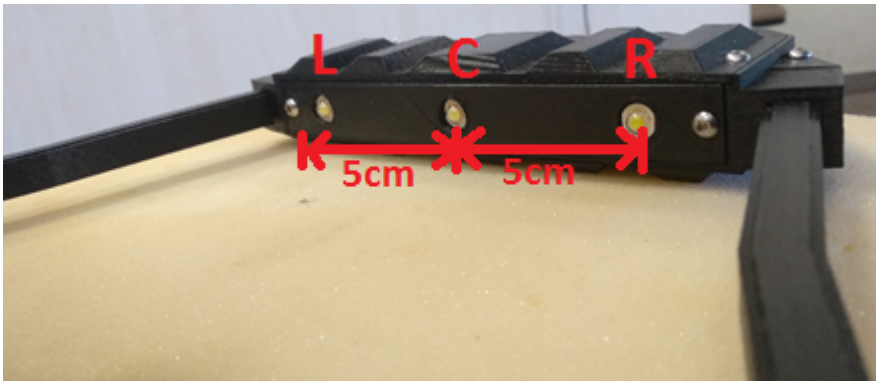

Figure 2.5: The array of three LEDs (marked as L, C, and R) mounted on the 3D printed headset

In the proposed BCI system, these LEDs are driven by a small current i.e. 13.3 mA for each LED in the ON state. Since they are driven by square waves with 50% duty cycle or by pseudo-random code having nearly equal number of zeros and ones, the average current for each LED becomes 6.65 mA amounting

to the total current of about 20 mA. This current requirement is fulfilled using the battery as mentioned in section 2.1.1.

2.1.3 Stimulator Circuit

The basic job of the stimulator circuit is to drive the three LEDs described in 2.1.2. There are two types of visual stimuli required depending on the type of VEP modality (f-VEP or c-VEP) used for classification. So, the two different stimulation signals are generated by designing a programmable stimulator circuit. The details of its hardware and software parts are discussed in the following paragraphs:

2.1.3.1 Programmable hardware Circuit

It is a microcontroller based circuit used to generate the drive signals for the stimulator LEDs. It employs Atmel $ATMEGA328P$ microcontroller which is a high Performance, Low Power, 8-Bit, AVR Microcontroller. It is available in 28-pin DIP (dual in-line package) and 32-pin TQFP (thin quad flat package) packages. It is also used in Arduino UNO which is a very popular open source, programmable, prototyping platform. We have used 32-pin TQFP package as shown in Figure 2.6.

Figure 2.6: ATMEGA328P microcontroller chip in 32-pin TQFP package

Some of the main features of $ATMEGA328P$ microcontroller are listed below:

a. It has advanced RISC (Reduced instruction set computing) architecture having 131 powerful instruction. Most of these instructions are executed in single clock cycle time

b. Its throughput can go up to 20 million instruction per second (20 MIPS) at 20 MHz clock

c. It has two 8-bit timers and one 16-bit timer with separate pre-scalar and compare modes.

d. It has three options to communicate with other devices: (i) programmable serial USART (Universal Synchronous Asynchronous Receiver Transmitter commonly known as RS232),(ii) Master/slave SPI (Serial Peripheral Interface), and (iii) 2-wire I2C (Inter-Integrated Circuit) interface

e. It has built-in Power-on reset and internally calibrated $8MHz$ oscillator

f. It has 23 programmable input output (I/O) lines. It also has 8 channel, 10 bit resolution analog to digital converter which can achieve maximum sampling rate of 9615 samples/s at 16 MHz clock.

g. It can operate from $1.8V - 5.5V$ DC power supply

Since the microcontroller can be powered up by $1.8 - 5.5V$ DC supply and we have used $6V - 8.4V$ DC battery as stated in 2.3, a low cost, linear voltage regulator (LM7805) is used to provide fixed $5\,V$ to the microcontroller. A 16 MHz quartz crystal is also used with the microntroller to provide external clock source for its smooth operation. The complete schematic design of the programmable hardware circuit for the stimulator is shown in Figure 2.7.

The programmable microcontroller based circuit is not only responsible for the generation of drive signals for the LEDs but also for the generation of synchronous marker signal in case of c-VEP stimulation. The led "L" is driven by the microcontroller's pin $PD6$, LED "C" by $PD7$ and LED "R" by $PD5$. The synchronous

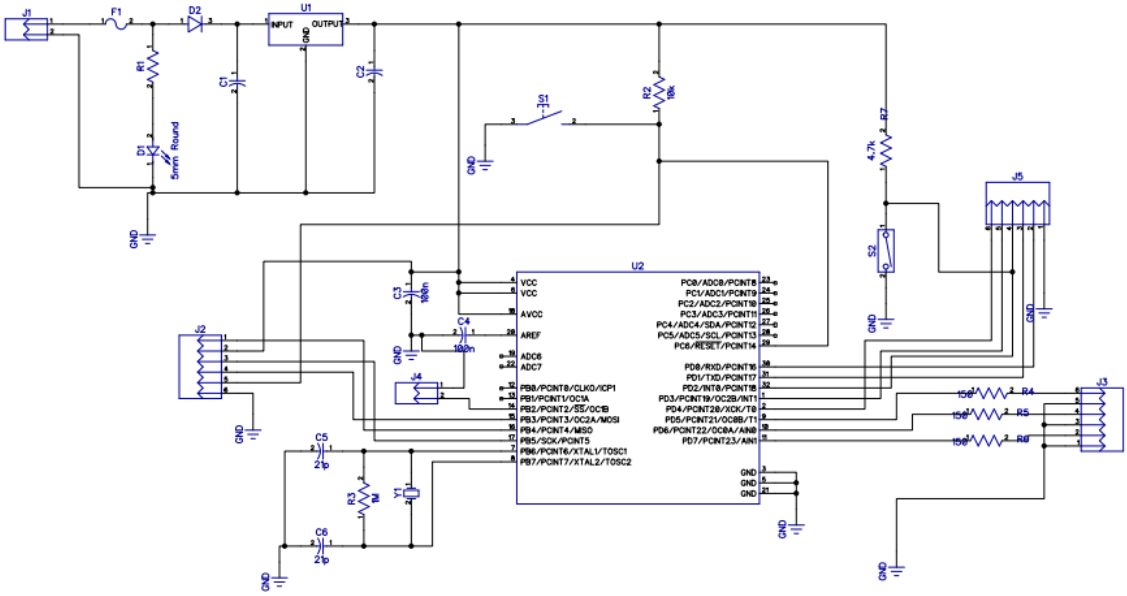

Figure 2.7: Schematic of the stimulator circuit

c-VEP marker signal is generated at the pin $PB2$ of the microcontroller. A select button (ON/OFF) is integrated with the $PD2$ pin of microcontroller in pull-up configuration to select among the f-VEP or c-VEP stimulus generation. The provision of 4 extra digital I/O pins is also provided in the stimulator hardware design for future utility. These extra I/O pins will provide the ease to extend the system from 3-target to 7-target system.

The circuit's schematic is converted into a single sided PCB layout using a free PCB design tool named as DipTrace. The PCB layout is given in Figure 2.8.

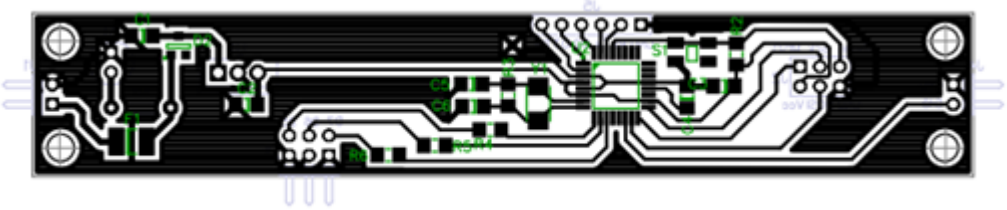

Figure 2.8: Layout of the stimulator circuit using DipTrace

The PCB layout was then printed using prototype PCB printing facility of Bilkent University's EEE department. The printed PCB is shown in the Figure 2.9.

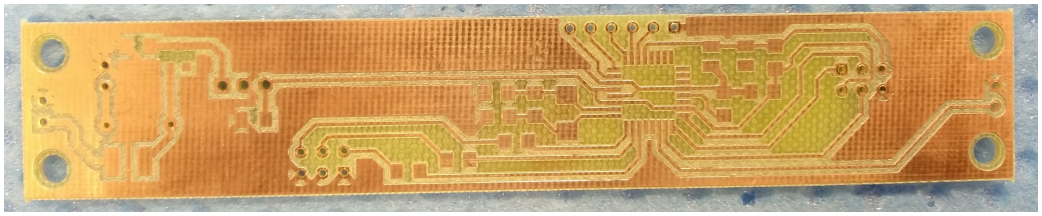

Figure 2.9: The stimulator circuit layout printed on a PCB

The PCB is 120 mm long and 21 mm wide. The final shape of the PCB after soldering of all the components is shown in Figure 2.10.

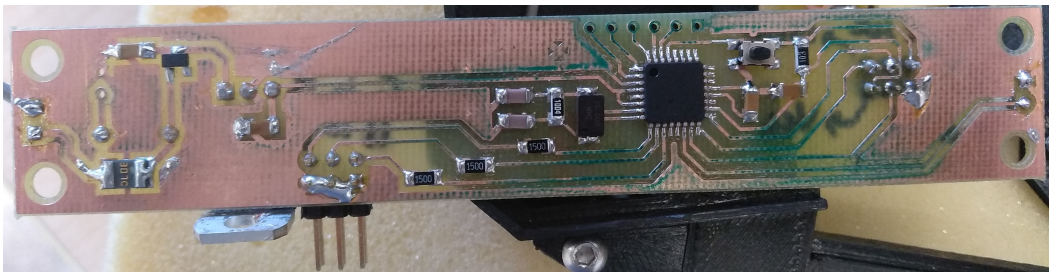

Figure 2.10: The stimulator circuit implemented on a 120 $mm \times 21$ mm PCB

2.1.3.2 Microcontroller programming for f-VEP Stimulation

f-VEP is a type of SSVEP paradigm in which each target flickers at different frequency and the brain generates the EEG activity in visual cortex having fundamental stimulus frequency and its harmonics. It has been discussed in detail in 1.1.3.4.

Since the proposed BCI system is a three target system, three signals having frequencies corresponding to the time periods of 50 ms, 44 ms and 38 ms are generated using the microcontroller. For the time periods to be exactly the integer multiples of of 1 ms, we have used timer interrupt which is running at 1 KHz i.e. it interrupts after every 1 ms. So we keep track of the timer interrupts and toggle the relevant digital I/O pins after corresponding half time period i.e. 25 ms, 22 ms and 19 ms. So the frequencies generated are 20 Hz, 22.73 Hz and 26.32 Hz and they are taken out from $PD6$, $PD7$ and $PD5$ pins of the microcontroller respectively. The programming code is written in an open source integrated

development environment (IDE) provided in Arduino-1.8.5. The source code is provided in the CD attached to this thesis whose contents are explained in Appendix B.

The OFF state of the button present at the outer body of the stimulator will signal the microcontroller to generate f-VEP stimulation signals. These signals are measured using the oscilloscope for verification purpose. The snapshots of the oscilloscope screen are shown in Figure 2.11.

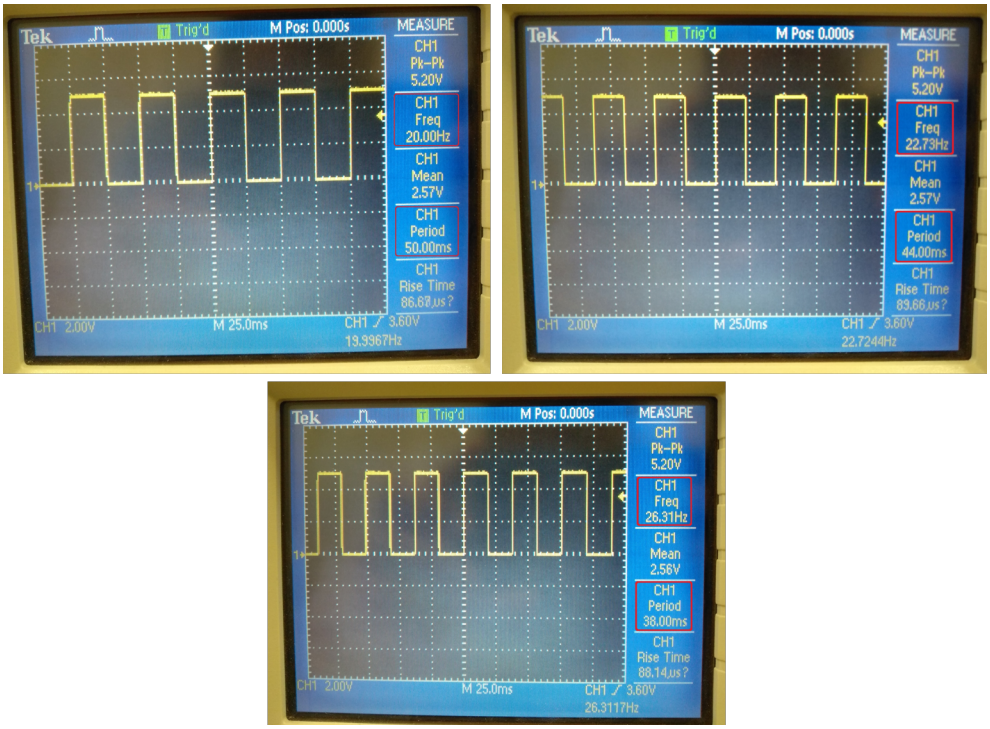

Figure 2.11: The oscilloscope screen shots showing LED drive signals for f-VEP stimulation (20 Hz, 22.73 Hz, *and* 26.32 Hz square waves)

2.1.3.3 Microcontroller programming for c-VEP Stimulation

In case of c-VEP modality, the stimulus signal is a pseudo-random code (array of 1's and 0's) instead of a single frequency. It is noted in the literature that maximum length sequence (m-sequence) is the most commonly utilized sequence in c-VEP based BCI systems [43]. A binary m-sequence can be generated by the

use of shift registers having maximal linear feedback. It is very useful in the c-VEP based BCI systems because its autocorrelation function is very close to the unit impulse function and it is found to be nearly orthogonal to its time shifted versions [43].

We have generated a 15 bit binary m-sequence using MATLAB (code is given in the attached CD). The generated sequence is "100110101111000". This is the code for one LED. The codes for other two LEDs are obtained by circularly shifting the above sequence by 5 and 10 bits respectively. So the three codes for the LEDs are:

a. m-sequence1 = 100110101111000

b. m-sequence2 = 110001001101011

c. m-sequence3 = 010111100010011

The correlation between these sequences is -0.0714, which is much close to zero meaning that all the three sequences are very close to being uncorrelated/orthogonal. In the proposed design of microcontroller code, the bit length is set as 10 ms which means that the 15 bits code will take 150 ms time. These three sequences are generated on $PD6$, $PD7$ and $PD5$ pins of the microcontroller driving L, C and R LEDs respectively by using timer interrupt running at 1 KHz. So each bit of the code is sent out to the respective I/O pin after 10 interrupts. A 6 ms long marker pulse is also generated at the $PB2$ pin of the microcontroller at the onset of each 15-bit m-sequence. The microcontroller code for the generation of these m-sequences is given provided in the attached CD (details about CD are given in Appendix B).

The ON state of the button present at the outer body of the stimulator will signal the microcontroller to generate c-VEP stimulation signals. These signals are measured using the oscilloscope for verification purpose. The screen-shots are given in Figure 2.12.

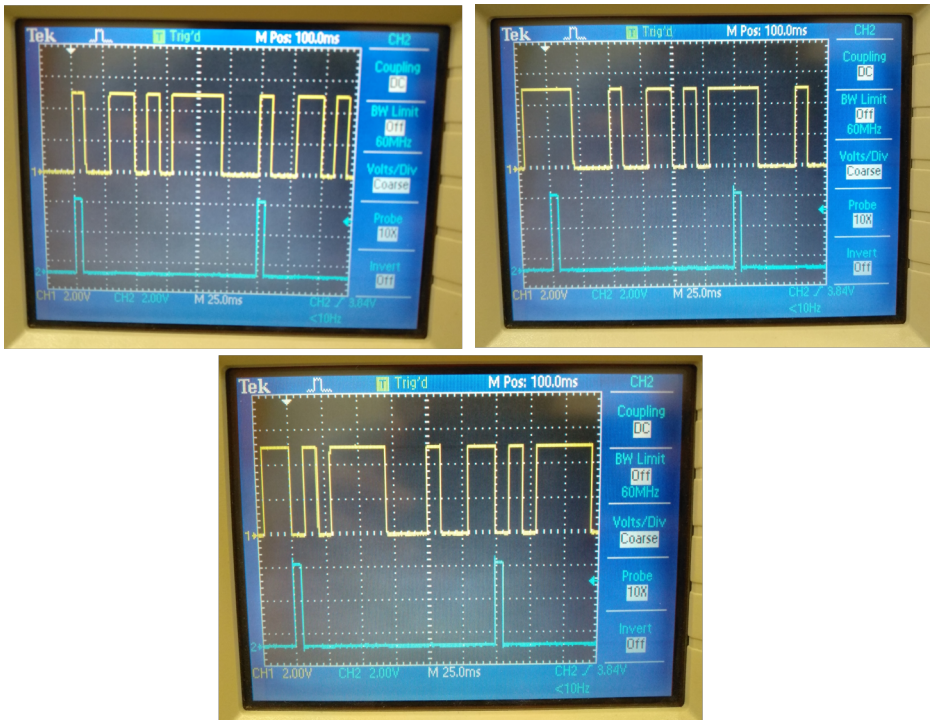

Figure 2.12: The oscilloscope screen shots showing LED driving drive signals for c-VEP stimulation (three pseudo-random m-sequences)

2.2 Dry Active Electrodes

There are two major types of electrodes being used for EEG recordings called dry electrodes and wet electrodes. As is clear from the names, the dry electrodes do not need any conductive gel between the skin and the metal body of the electrode while wet electrodes need such gel.

As the EEG signal amplitude is of the order of few μV , the transportation of this signal to the data acquisition hardware becomes very difficult because little interference coupling to the cables carrying these signals may ruin the signal. 50/60 Hz line's capacitive coupling with the subject's body is also present to interfere with the signal. So, it becomes a challenge to transport the poor EEG signal from the electrode to the data acquisition system. These interferences can be mitigated by the use of wet gel electrodes but they have their own limitations. In other words, they cannot be used for long term recordings as the signal quality goes low as the gel dries out [83]. Also, the wet gel produces discomfort to the

subject and repetition of experiments becomes difficult due to exhaustive skin preparation procedures [83] and post experiment washing activities.

To overcome these problems, active electrodes (AE) are suggested in the literature [84],[85],[86]. An active electrode (AE) locally amplifies/buffers the μV level EEG signal before driving any cabling. These buffers/amplifiers are put just next to the skin electrode contact minimizing the path between the skin and the active circuit. This minimal path length mitigates/minimizes the line interference [83]. The low output impedance of an AE mitigates cable artifacts [83] thus enabling the use of high-impedance dry electrodes for greater user comfort.

In the proposed BCI system, we have used Ag/AgCl dry electrodes from OpenBCI with a unity gain amplifier (buffer). From now on, the buffer circuit will be called as active circuit. So, combining active circuit with the dry electrode makes the dry active electrodes (DAE). The active circuit is built by using the circuit shared in OpenEEG project (a free platform to share the ideas to build low cost EEG devices "http://openeeg.sourceforge.net/doc/"). Both of these parts are explained in the upcoming paragraphs.

2.2.1 Dry electrodes

In the proposed BCI system, Ag/AgCl dry electrodes from openBCI (an open source biosensing tools manufacturer "https://openbci.com/") are used. Figure 2.13 shows the dry electrode in parts and in assembled form.

2.2.2 Active Circuit

As we have mentioned above that the active circuit is used next to the skin electrode contact to keep the signal integrity intact and get rid of the application of wet gel. The design of the active circuit is quite simple because it is just a unity gain amplifier called buffer. As mentioned earlier, the circuit design of the active circuit is taken from OpenEEG project which provides free techniques

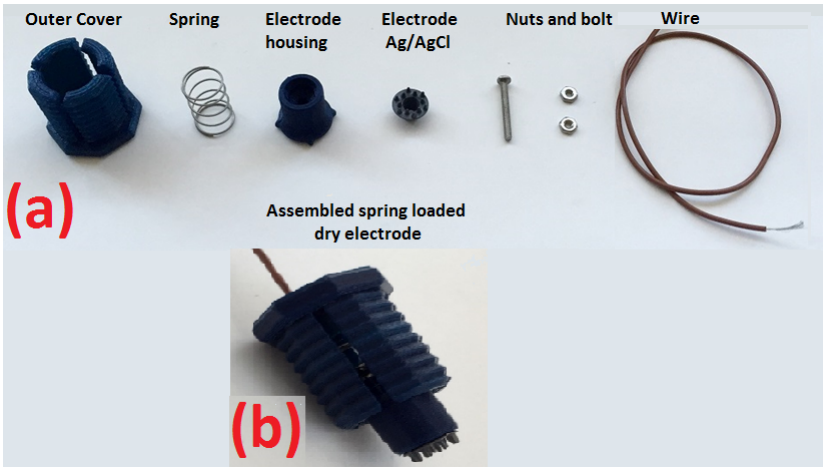

Figure 2.13: A sample of dry electrode from OpenBCI (a) shows the individual parts and (b) shows the assembled form of the spring loaded dry electrode

to design low cost EEG devices at home. The buffer design uses Texas Instrument's TLC272 op-amp which is a low noise, high input impedance precision operational amplifier. It also provides good CMRR (typically 80dB). The active circuit schematic is given in Figure 2.14.

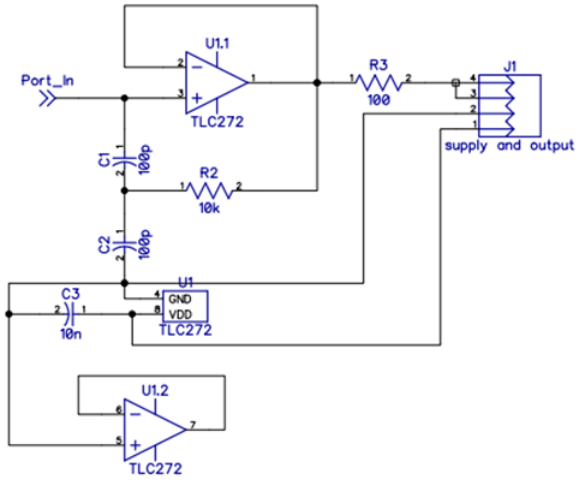

Figure 2.14: Schematic of the active circuit (a unity gain amplifier implemented using TL272 op-amp). The bottom op-amp(U1.2) is of no use in the ciruit. It is placed because the IC package has two op-amps.

The schematic is then converted to a small circular PCB (25 mm diameter) layout using free PCB design tool "DipTrace". The PCB layout and its actual

shape is shown in Figure 2.15.

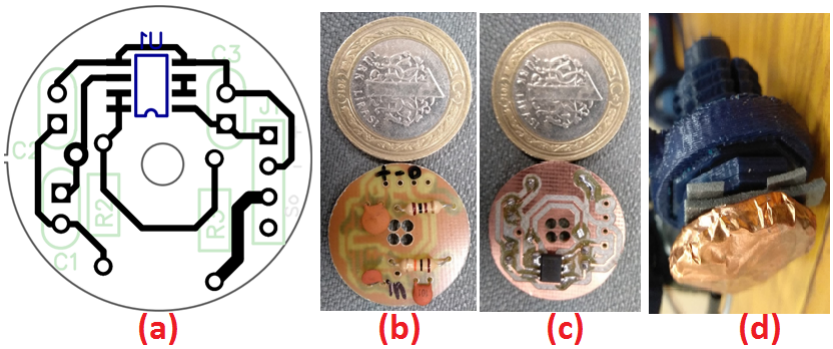

Figure 2.15: (a) Active circuit layout (b) active circuit PCB (top view) (c) active circuit PCB (bottom view) (d) The complete dry active electrode having dry electrode and active circuit wrapped in thin copper sheet to provide shielding to the circuit

2.3 EEG Data acquisition hardware

In the proposed BCI system, a 4-channel, battery powered EEG data acquisition hardware is designed which can support sampling rates ranging from 250 to 2000 samples/sec for each channel. It can be further divided into four subsections as follows:

a. EEG Amplifier Unit

b. Microcontroller unit

c. Wifi Transmitter and Receiver

d. Power supply unit

All of these parts are discussed in detail in the following subsections:

2.3.1 EEG Amplifier Unit

The EEG amplifier unit is the first interface of the EEG signal with the data acquisition hardware after the active electrode and some cables. The purpose of this unit is to amplify the poor EEG signal to some extent and digitizes it using analog to digital converter. At this stage, the analog EEG signal is converted into digital domain and is forwarded to the next stage. Since the EEG signal is accompanied with a lot of noise and unwanted artifacts, the incoming signal is first passed through a first order passive low pass filter (built up by capacitor and resistor) and then amplified by giving a small gain of 24. The EEG signals are acquired as differential signal to get rid of the common mode unwanted signals. All of these characteristics are combined in a single EEG acquisition chip $ADS1299$ manufactured by Texas Instruments. In our proposed BCI system, 4-channel version of the chip i.e. $ADS1299-4$ is used for the EEG signal acquisition. Some of the main features of this chip (referred to as "EEG chip" throughout the document) are listed below:

a. It has four low noise programmable gain amplifiers (PGAs) whose gains can be adjusted as one of the values from 1, 2, 4, 6, 8, 12, or 24.

b. It has 4-channel, simultaneous sampling, analog to digital (A/D) converter having 24-bit resolution

c. It can sample the signals at sampling rates of 250, 500, 1000, 2000, 4000, 8000 or 16000 samples/second

d. It provides very high common mode rejection ratio (CMRR) of $-110\ dB$.

e. It can use external as well as internal reference for A/D conversion.

f. It has built in oscillator to provide clock source to the circuit internally

g. It can use unipolar as well as bipolar supplies. Since it is mixed signal device, its analog side needs $4.75-5.25\ V$ and digital side needs $1.8-3.6\ V$ supplies.

h. It gives digital data output through serial peripheral interface (SPI)

i. It has the provision to connect the input channels to the internally generated test signals, temperature measurement or lead-off detection.

i. It is available in 64-pin Thin Quad Flat Package (TQFP).

The real look of the EEG chip (64-pin TQFP chip) is given Figure 2.16

Figure 2.16: The 4-channel EEG data acquisition chip (ADS1299-4) in 64-pin TQFP package

2.3.2 Microcontroller Unit

The purpose of the microcontroller unit in this section is to collect the data from EEG chip using SPI protocol and forward them to the wifi transmitter module. We have used Atmel ATMEGA328P microcontroller to configure the EEG chip for certain parameters like sampling rate, start and stop data acquisition. The microcontroller is also responsible for the communication with EEG chip and Wifi transmitter. The key features of the microntroller are discussed in section 2.1.3.1.

The microcontroller needs to communicate with the EEG chip but the microcontroller works on 5V logic level while EEG chip's digital side works on 3.3V logic level. So, a logic level shifter chip (Texas Instrument's SN74LVCC3245ADW) is used between the microcontroller and the EEG chip for reliable communication.

The microcontroller is supposed to (i) configure sampling rate, start and stop of the data conversion, setting the gain of the EEG amplifiers, connecting input

channels with the desired functionalities (ii) receive digital EEG data output from the EEG chip. It configures and controls the EEG chip by sending some commands to the EEG chip or writing to some of its internal registers. The complete details are available in the datasheet of ADS1299 chip (provided in the attached CD). Some important configurations which we have used in our design are described as follows:

a. It can control the EEG chip by sending start, stop or reset commands. These are single byte commands which the EEG chip can understand and act accordingly. It sends 00001000 to start, 00001010 to stop, and 00000110 to reset the EEG chip. The commands are sent using SPI protocol at 8 MHz clock generated by the microcontroller.

b. For the selection of sampling rate, the microcontroller writes some values to the "CONFIG1" register of the EEG chip. This register is located at 01 hex location of the EEG chip and needs 96 hex to set 250 $samples/sec$ (SPS), 95 hex for 500 SPS, 94 hex for 1000 SPS, and 93 hex for 2000 SPS. We have tested our system for a maximum of 2000 SPS.

c. There are separate registers to configure the signal connections of each analog input channel and setting their corresponding amplifier's gain. These registers are named as "ch1set", "ch2set", "ch3set" and "ch4set". They are located at register addresses of 05 hex, 06 hex, 07 hex, and 08 hex respectively in the EEG chip. They are given the value of 68 hex for the connection of the respective input channel to the standard EEG electrodes while they get the value of $6D$ hex if we want to connect them to the test signal. These values are calculated by fixing the PGA gains at 24.

d. The test signal parameters are configured by setting the "CONFIG2" register located at 05 hex address in the EEG chip. "CONFIG2" register is given the value of $D4$ hex for the internally generated test signal having frequency equal to the clock frequency divided by 2^{21}.

The second part of the microcontroller's communication with the EEG chip is to receive the digital data through SPI. The EEG chip outputs the data in the

form of 15 byte array. This array contains 3 bytes of status registers and 3 bytes for each of the four channels data. To get this data, the microcontroller waits for the DRDY pin of the EEG chip to get low. As soon as it detects the falling edge of the DRDY pin it makes CS pin low and starts generating an 8 MHz SCLK signal. The EEG chip then clocks out the data on rising edge of SCLK.

We have used OpenBCI's arduino based library to develop the code for the microcontroller to communicate with the EEG chip (the library files are provided in the attached CD). The microcontroller's program to communicate with the EEG chip is written in Arduino-1.8.5 IDE (the source code is also provided in the attached CD explained in Appendix B). Figure 2.17 shows the timing diagram (taken from the datasheet of the ADS1299 chip) of the communication protocol to exchange data with the EEG chip .

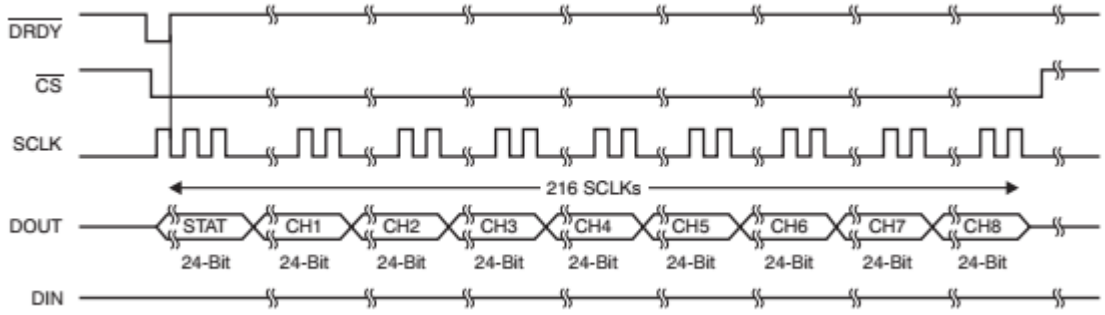

Figure 2.17: The timing diagram of the communication protocol used to exchange data with the EEG chip (ADS1299)

When the microcontroller receives this data, it forwards it to the wifi transmitter module using standard RS232 serial communication protocol at the baud rate of 1 Mbps.

2.3.3 Wifi Transmitter and Receiver

Since we have proposed a wireless BCI system, a wifi communication is used to forward the EEG data to DPU. ESP8266 wifi transceiver board which is an open source Arduino based prototyping platform is used as wifi transmitter (wifi Tx)

module. On the receiving side, "Node-microcontroller" which is also an Arduino compatible open source, prototyping platform is used as wifi receiver (wifi Rx) module. The Node-microcontroller is also an ESP8266 based wifi transceiver having an additional feature of built-in serial to Universal Serial Bus (USB) conversion to communicate with the computer. The node microcontroller and the ESP8266 wifi module are shown in Figure 2.18.

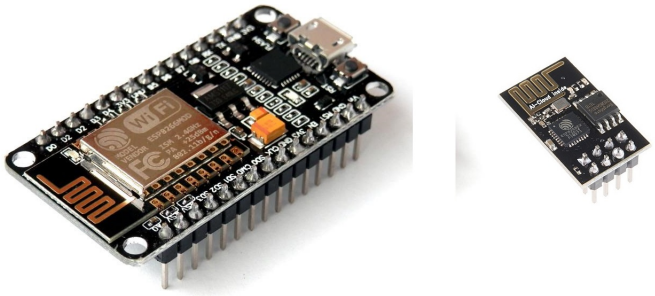

Figure 2.18: Real look of the node microcontroller (node MCU) used as wifi Rx module and ESP8266 wifi module used wifi Tx module in the proposed BCI system

The wifi Tx receives data from the microcontroller via RS232 at the baud rate of 1 $Mbps$, makes a packet of 960 bytes, and sends it to the remote wifi Rx via user datagram protocol (UDP). The wifi Rx receives this data packet and forwards it to the data processing unit (DPU) via RS232 serial communication at a baud rate of 230400 bps. This is the forward link of communication. The reverse communication link includes sending of command/s to the microcontroller via wifi transmitter module to start the data acquisition. Upon reception of this start command from the DPU, the microcontroller configures the EEG chip for the start of data conversion. In simple words, both the wifi modules are working as wifi-UART bridge.

Some of the key features of the ESP8266 wifi module are listed below:

a. It has 802.11 b/g/n support with built in PCB trace antenna.

b. It has Tensilica L106 32-bit processor having UART, SPI, and I2C communication protocols. It operates at 2.5-3.6 V DC supply and takes maximum of 80 mA current.

c. It has built-in TCP and UDP stacks which makes it much easier to implement these protocols.

d. It has been extensively used in arduino compatible open source prototyping platforms such as Node-microcontroller etc.

2.3.4 Power Supply Unit

The EEG data acquisition hardware is powered up by a 7.4 V battery. This battery is exactly same as the one described in section 2.1.1.

The EEG chip analog section and the microcontroller need 5 ± 0.25 V, while the digital part of the EEG chip needs 2.7 ± 0.9 V. The EEG chip also needs $-2.5V$ supply. The wifi transmitter module needs 3 ± 0.5 V. All these voltage requirements are fulfilled by placing different voltage regulators in front of the DC battery as described below:

a. $5\ V$ **regulator:** Texas Instruments' $LP2989IM-5.0$ IC is used which is a low noise and ultra low dropout voltage regulator giving $5\ V$ fixed output for up to 500 mA current. It is used to power up the microcontroller and analog side of the EEG chip. Also, its output serves as the input to all the other voltage regulator.

b. $3.3\ V$ **regulator:** Texas Instruments' $LP5907MFX-3.3$ is used. It is an ultra low noise, low drop out (LDO) voltage regulator, and provides fixed $3.3\ V$ output for load current of maximum 250 mA. It is used to power up the wifi transmitter module.

c. $-2.5\ V$ **regulator:** Texas Instruments' $TPS72325DBVR$ is used. It is a low noise, LDO, linear voltage regulator having negative output. It

is fed with $-5V$ input by using a Texas Instruments' voltage converter $LM2664m6$ which converts $5V$ to $-5V$. $-2.5\ V$ is required by the digital side of the EEG chip as we have used it in bipolar supply configuration.

d. $2.5\ V$ **regulator:** Texas Instruments' $TLV70025DDCR$ is used which is a low drop out voltage regulator having $2.5\ V$ fixed output for the maximum load current of 200 mA. Its output is also used by the EEG chip in its digital side.

2.3.5 Integrated EEG Data Acquisition Hardware

In the above subsections 2.3.1, 2.3.2, 2.3.3 and 2.3.4, all the parts of the EEG data acquisition hardware have been discussed in detail. These parts are all integrated together to make a single unit of EEG data acquisition hardware in the form of a PCB. The complete schematic is shown in the Figure 2.19. This schematic is entered in Altium schematic design tool.

The summarized list of major components used in this design are as follows:

a. ADS1299-4 (4-Channel EEG chip)

b. Voltage regulators as described in section 2.3.4.

c. SN74LVCC3245ADW (Logic Level Shifter)

d. Atmel ATMega328P-AU microcontroller

e. ESP8266 Wi-Fi Transmitter and node-microcontroller as wifi receiving module

f. 16 MHz quartz crystal to provide external clock source to the microcontroller

g. ESD protection diodes for circuit's protection

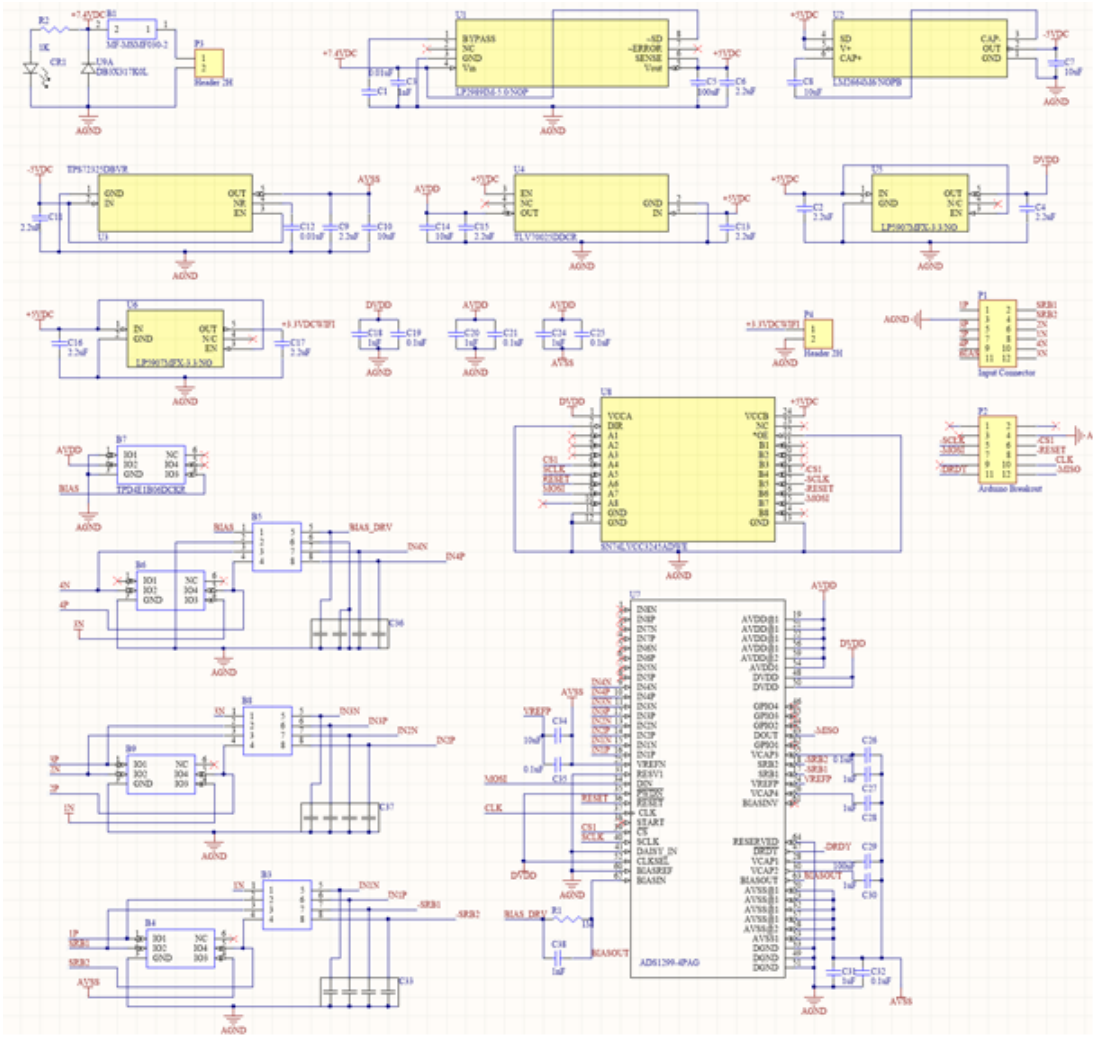

Figure 2.19: The schematic diagram of the 4-channel EEG data acquisition circuit

h. Push button for reset and ON/OFF button for power ON and OFF the circuit

i. Bunch of resistors, capacitors, connectors and other similar components

The schematic given in Figure 2.19 may be unreadable due to page margins. The readable view of the same is provided in the attached CD (explained in Appendix A).

The schematic is then converted to the double layer PCB layout using Altium

PCB design tool. The top and bottom views of the PCB layout are shown in Figure 2.20. In the layout design of this PCB, the two separate copper pours are used for digital ground and analog ground because it mounts a mixed signal device (ADS1299-4). The reason behind using separate analog and digital grounds is to prevent the noise sensitive analog side from the unwanted interference due to highly varying digital signals.

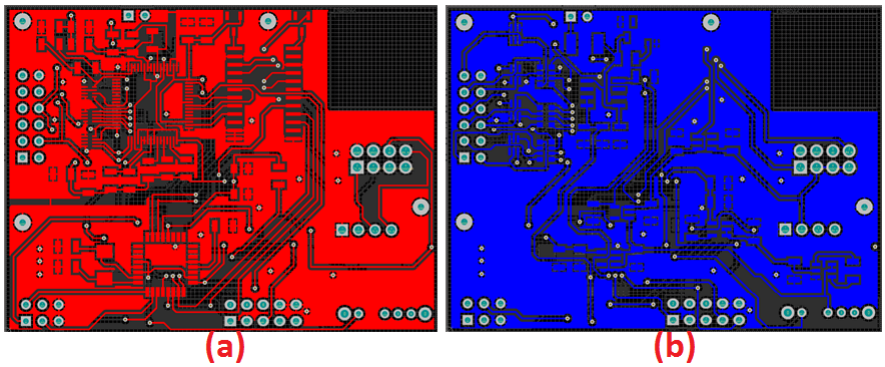

Figure 2.20: The PCB layout of the EEG data acquisition hardware (a) Top view (b) Bottom view

The PCB files were then sent to China for PCB manufacturing. The soldering process of the components was performed in the Bilkent University's EEE department. The final look of the PCB is shown in Figure 2.21.

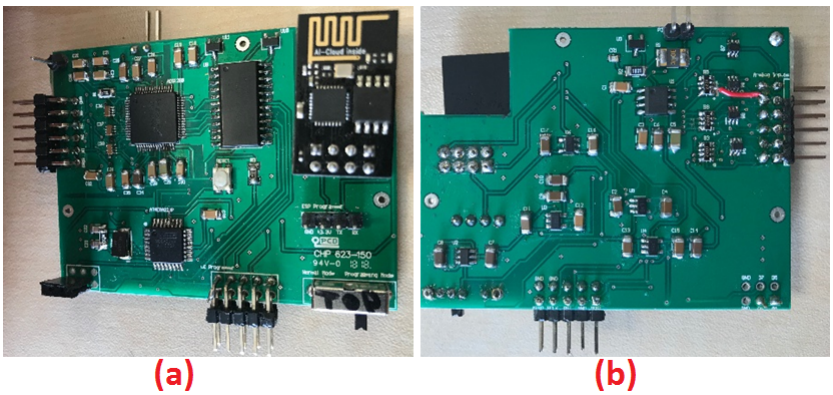

Figure 2.21: EEG data acquisition hardware circuit implemented on a double sided PCB (a) Top view (b) Bottom view

2.4 Data Processing Unit (DPU)

The data processing unit (DPU) is responsible to collect the raw EEG data through serial port of the computer, separates the data for individual channels, applies some processing techniques, displays the results and saves the data in hard drive. All these sub-units are implemented in MATLAB-R2018b and discussed in detail in the upcoming subsections.

2.4.1 Data Collection

The DPU first sends a byte long command containing an ASCII character ("$") to the wifi Rx module via serial port, which forwards the same character to the wifi Tx module. Upon reception of this symbol, the wifi Tx module pulls its $GPIO0$ pin to logic high which is detected by the microcontroller (ATMEGA328P). Then, the microcontroller configures the EEG chip to start the data conversion by sending commands as mentioned in section 2.3.2. After configuration of the EEG chip, the microcontroller starts collecting EEG data and forwards it to the wifi Tx module which waits until 960 bytes of data is accumulated. This amount of data is accumulated in 80 ms if the sampling rate is selected as 1000 SPS. The wifi Tx module sends this 960 bytes long packet to the wifi Rx module which forwards it to the DPU through RS232 at 230400 bps baud rate.

The above mentioned process starts with the creation of a serial port object corresponding to the computer's serial port to which the wifi Rx module is connected. The serial port is then configured for the baud rate of 230400 bps. The input buffer size of the serial port is set to 10 times the packet size of 960 bytes. Then, it sends the "$" character via this serial port object and waits for the data to come. The DPU waits until 12480 bytes (equivalent to 1.04 seconds @1000 SPS) get accumulated. It then saves this raw data on the hard disk in a comma separated text file with name of "rawEEG.txt" at the MATLAB working directory.

2.4.2 Separating the data for each channel

The raw EEG data received at the DPU end is in the form of a big chunk of 12480 bytes. The EEG chip samples the four analog input channels simultaneously with 24 bit (3 bytes) resolution, so that each sample contains 12 bytes, 3 for each channel. It means that the data chunk of 12480 bytes contains $\frac{12480}{12} = 1040$ samples. In the MATLAB code, all the data is separated in the form of groups of 3 bytes (24 bits) each first. Since MATLAB does not have any 24-bit data type, these 24-bits are extended to 32-bits to fit with the standard data type. The EEG chip converts the data in the form of 2's compliment format. So, 24-bit channel data is converted to 32 bit data by plugging eight "zeros" before the data if its MSB (most significant bit) is 0 or eight "ones" if MSB of the 24-bits is 1. At this stage, each sample of 12 bytes has been converted into 4 int32's (int32 is a 32 bit MATLAB signed integer data type). Then, the data is separated for each of the channels by picking first 32-bit integer from each sample for channel1, second from each sample for channel2 and so on. Finally, these values are multiplied by a number 2.235×10^{-2} to convert the samples into μVolt values. The number 2.235×10^{-2} comes from EEG chip datasheet which is calculated by using the following equation:

$$LSB\ value\ (in\ Volts)\ =\ \frac{2 \times \frac{V_{ref}}{Gain}}{2^{24}} \tag{2.1}$$

LSB stands for least significant bit of the data. V_{ref} is the difference of voltages measured at pin24 (V_{refP}) and pin25 (V_{refN}) of the EEG chip. It is measured as $4.5\ V$ in our designed circuit. The "Gain" refers to the gain of the PGAs of the EEG chip which is set as 24 in our design. 2^{24} comes from the 24 bit resolution of the A/D converter of EEG chip. So,

$$\begin{aligned} LSB\ value\ (in\ Volts)\ &=\ \frac{2 \times \frac{4.5}{24}}{2^{24}}\ =\ 2.235 \times 10^{-8} \\ LSB\ value\ (in\ \mu Volts)\ &=\ 2.235 \times 10^{-2} \end{aligned} \tag{2.2}$$

After this step, data becomes ready for further processing discussed in the next subsections.

2.4.3 f-VEP data processing and display of results

As mentioned earlier in the section 2.1, the stimulator LEDs are driven using three square wave signals of different frequencies in case of f-VEP experiment. The left LED flickers at 20 Hz, the center at 22.73 Hz and the right LED flickers at 26.32 Hz. The waveforms driving these LEDs are made sure to have integer milliseconds of time periods. So the left, center and right LEDs flicker with time periods of 50 ms, 44 ms and 38 ms respectively.

In the proposed BCI system, the sampling frequency of the EEG chip is set as 1000 SPS for the experiments which means that each sample is taken after every 1 ms. In real time, the DPU collects 1.04 seconds data chunk from the wifi Rx module through serial port, combines this data with the previous 2.08 seconds data making it a total of 3.12 seconds data length ($3.12 \times 1000 = 3120$ *samples*).

For f-VEP experiments, the data from only one channel is needed so that data coming from any of the three channels is selected for further processing. The DPU chooses a sliding window of length 1040 samples and slides it over the entire 3120 samples long data for all the three time periods one by one. This process gives three matrices of dimensions 41×1040, 47×1040 and 54×1040 for the stimulator waveforms' periods of 50 ms, 44 ms *and* 38 ms, respectively. Then, averaging over first dimension of all the three matrices is taken. After averaging, these matrices become 1×1040 arrays (named as A1, A2 and A3). A1 will have only 20 Hz and its harmonics, A2 will have 22.73 Hz and harmonics, and A3 will have 26.32 Hz and harmonics. The spectral powers (SP)of these arrays are measured around their respective frequencies and their two harmonics (Let's denote them as $SP1$, $SP2$ *and* $SP3$ respectively). The maximum of these three spectral powers enables the DPU to decide about the user's focus in real time.

$$
\begin{aligned}
SP1 &= SP(A1\ in\ [19\ 21], [39\ 41]\ and\ [59\ 61]\ Hz\ bands) \\
SP2 &= SP(A2\ in\ [21.73\ 23.73], [44.46\ 46.46]\ and\ [67.19\ 69.19]\ Hz\ bands) \\
SP3 &= SP(A3\ in\ [25.32\ 27.32], [51.64\ 53.64]\ and\ [77.96\ 79.96]\ Hz\ bands)
\end{aligned} \tag{2.3}
$$

On the basis of spectral powers of the individually averaged arrays, the DPU takes the decision whether the subject is focusing at L, C or R LED.

$$
\begin{aligned}
decision &= L\ if\ max(SP1, SP2, SP3) = SP1 \\
decision &= C\ if\ max(SP1, SP2, SP3) = SP2 \\
decision &= R\ if\ max(SP1, SP2, SP3) = SP3
\end{aligned} \tag{2.4}
$$

All the above mentioned processes are summarized in a cyclic flow diagram shown in figure 2.22.

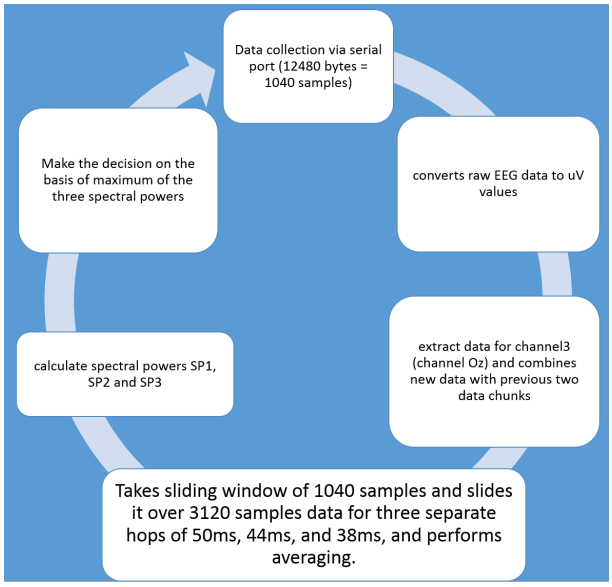

Figure 2.22: All the steps of data processing in case of f-VEP experiments shown as a cyclic process

The DPU displays all the three spectral powers on a same graph in real time. The first value of the graph is shown at 3.12 seconds from the start of the experiment, and it keeps updating the graphs every 1.04 seconds. The decisions are also displayed as the string of characters made up of L's, C's and R's. This string is also updated after every 1.04 seconds. The real time EEG signal from the input channel (selected using the drop down menu "input channel") and its spectrum without averaging is also shown on the GUI screen. All of these displays are discussed in detail in section 2.4.6.

2.4.4 c-VEP data processing and display of results

The initial steps of data collection and data separation in this case are the same as those of f-VEP case. Contrary to the f-VEP, c-VEP experiments need separate training session for each subject before going to actual decision making process.

As described earlier in section 2.1, we used 15 bits m-sequence code for the c-VEP stimulator. The code is circularly shifted by 5 bits and 10 bits to make code for other two targets. Each bit of the code is 10 ms long making the whole code length as $150ms$. Keeping the EEG chip's sampling rate at 1000 SPS, EEG data corresponding to one code length is completely acquired as 150 samples. The stimulator also provides the marker signal at the onset of each code.

For training session, EEG data from all the three channels is acquired for 200 code repetitions which means that data is acquired for 200×0.15 $seconds$ = 30 $seconds$. During the recording, the subject is asked to focus his/her gaze on the left LED which is driven by the original non-shifted m-sequence code. The fourth channel of the EEG data contains a marker indication, the onset of which points out the start of the code sequence. Therefore, in the DPU all the EEG data recorded during training session is received, converted to μV values, separated for all the four channels $O1$, $O2$ and Oz and the marker channel. Using the onset of the marker channel, the brain responses corresponding to each run of the m-sequence code are extracted for all the three EEG channels. These

brain responses are averaged over number of trials (number of runs of the m-sequence). The resulting averaged data forms a 3×150 matrix having averaged brain response of the three EEG channels. The averaged data from one of the three channels is selected as the target template (name it as "template1") for the left LED ("L"). The templates for other two LEDs ("C" and "R") are obtained by circularly shifting the "template1" by 50 samples ($5\times$ bit length in ms $\times$ sampling frequency in samples/ms) and 100 samples ($10\times$ bit length in ms $\times$ sampling frequency in samples/ms), respectively. This method is applied due to the fact that the other two LEDs are flickering by the time lagged versions of the m-sequence running on the left LED. The three templates are stored in a file in hard drive. The training process is summarized in the figure 2.23.

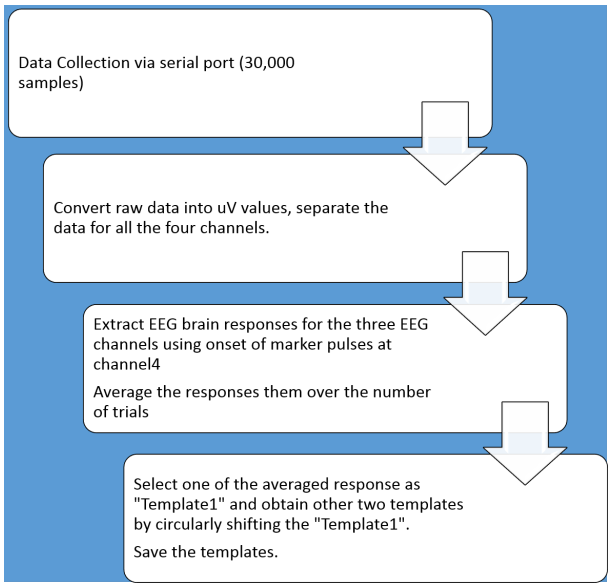

Figure 2.23: All the steps of data processing performed in the training stage of c-VEP experiments shown as a process

After training session is complete, the real time online experiment can be started. In this case, the DPU collects EEG data for 1.05 *seconds* corresponding to 1050 *samples* which is equivalent to the time to completely run 7 code sequences. Then, samilar to the training process, raw EEG data is converted into μV values and separated for all the four channels. Then, the EEG brain responses to the individual code run are extracted for three EEG channels with the help of marker indications available at channel4. These brain responses are

averaged over number of trials (no. of code runs which are 7 for 1.05 s recording). The DPU takes one of channel's averaged response as test signal and correlates it with the templates saved in the training session. The maximum correlation will be found with the template corresponding to the target at which the subject is focusing his/her gaze. The online cVEP process is summarized in the figure 2.24.

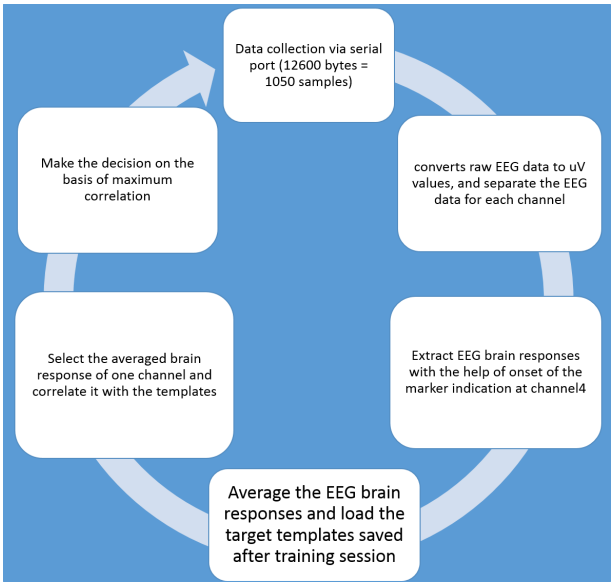

Figure 2.24: All the steps of data processing performed in test stage of c-VEP experiments shown as a cyclic process

2.4.5 Extracting the Final Message String

As it has been discussed in 2.4.3 and 2.4.4, the decision (L, C, or R) is taken after every recording. The recording time can be set using the GUI window under the heading "time/recording". There is a chance of making error in estimating the current gaze on the basis of short recorded data (normally 1.04 sec or 1.05 sec). These errors can be neglected and the final decision string is built up using the number of decisions. The final message string will help build the application interface which can decode it and perform some control tasks such as home appliances control. The extraction of final string from the live decision-string can be performed using either synchronous or asynchronous method as described below:

2.4.5.1 Synchronous Method

In the synchronous method, we have used sound beeps after certain number of recordings as a clue for the subject to synchronize his/her gaze changes. The sound parameters like frequency, volume and delay between two sound beeps (say "beep delay") can be selected using the GUI. Once the beep delay is set, it cannot be changed during the experiment. The first beep means that the data acquisition has been started.

From the decisions made during two consecutive beeps, the maximum occurring decision is chosen as the final decision. For instance, if two consecutive final decisions are "L" which means that the subject looked at left LED for two beep delays, the final string starts by printing 'S'. After printing 'S', it gets updated from the final decisions on the basis of maximum occuring live decisions in one beep delay.

For example, if the beep delay is 5, it means that there will be 5 live decisions between two consecutive beeps. If the live decisions in one beep delay are "LCLLC", the final message will take it as single "L" as it has occured thrice while "C" occured twice and there is no "R". If there are two consecutive L's in the final decision, it will start the final message string. The example showing live decisions and the final message string is shown in Figure 2.25.

2.4.5.2 Asynchronous Method

In the asynchronous method of extracting the final message string from the live decisions, sound beeps are not used. In this method, the subject may count in his/her mind to change the gaze. In our system, the final message string starts if there are at least 7 L's in the last 10 decisions. Once the final message string is started, it keeps looking for the change in the current decision from the previous one. Whenever there is a change in the live decision, it counts the previous consecutive live decisions. On the basis of the count, it decides to put one, two, or three L's, C's, or R's in the final message string. If the count is between 3

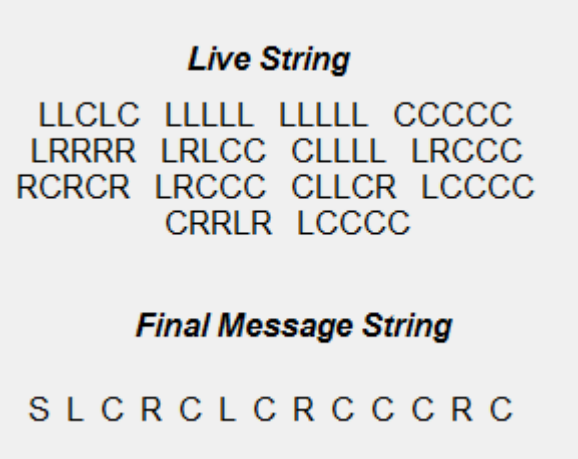

Figure 2.25: Extraction of final message string from the live decisions using synchronous method

and 7, it inserts one corresponding letter. If it is between 8 and 12, it inserts two letters. If it is between 13 and 17, it inserts three letters and so on. An example of such implementation is shown in Figure 2.26.

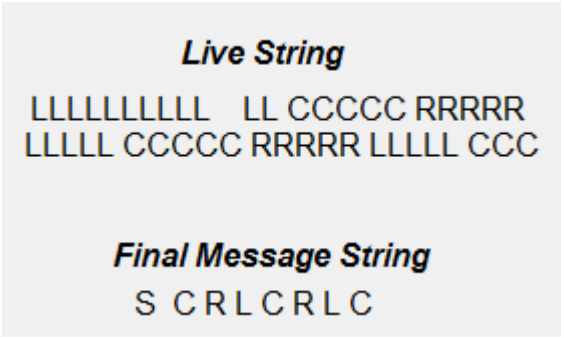

Figure 2.26: Extraction of final message string from the live decisions using asynchronous method

2.4.6 Graphical User Interface (GUI)

All the functions and processes mentioned in the above subsections 2.4.1, 2.4.2, 2.4.3, and 2.4.4 are written as MATLAB scripts and on top of all these functions, a graphical user interface (GUI) is designed in MATLAB to provide click and select control to the user. The GUI provides the user the facility to select between the online and offline analysis of the data. In case of offline data analysis, the user

gives the GUI the path of the previously saved raw EEG data file (*.txt). On the other hand, in case of online analysis, the GUI program takes the raw EEG data from the wifi Rx module through serial port. Once the data collection is done, the data separation for the channels and conversion into microvolt values is done and then other processing techniques are applied as per the selection of the user.

The GUI takes the number of recordings and time per unit recording in seconds as the inputs from the user. The user can also select one out of the four functions: (i) f-VEP online/offline (ii) c-VEP training (iii) c-VEP online/offline (iv) Monitoring. These options are provided in the form of buttons. As is clear from the names, upon pressing f-VEP button, the f-VEP online/offline based analysis discussed in subsection 2.4.3 is done. Similarly, the second button starts c-VEP training process and the third one starts the online/offline c-VEP analysis process. The last button called "monitoring" provides only the display of real time EEG signals from all the three EEG channels. This monitoring process only contains data collection, conversion into microvolts values, separation for each channel and displaying the data in real time. These steps are exactly the same as those discussed in subsections 2.4.1 and 2.4.2. The detailed procedure to use the GUI is given in chapter 3. The sample GUI window after completion of one of the experiments is shown in Figure 2.27.

Figure 2.27: A sample GUI window after completing a c-VEP experiment

2.5 3D Printed Headset

Since the proposed BCI system is wearable, a headset mounting all the parts of the system except the DPU is developed using 3D printing technology. In this technology, three dimensional objects are printed by adding the material layer by layer according to the computer aided designed (CAD) models. All this CAD design and printing process is done by "ARTI BOYUT", a Bilkent University's cyberpark company.

The headset provides five locations according to the 10-20 internal system (O1, O2, Oz, FCz and FPz) for the Spring loaded dry electrodes (explained in section 2.2.1). It also provides the space for the placement of active circuits (circular PCBs of 25 mm diameter) just near the dry electrodes. Figure 2.28 shows the O1, Oz and O2 electrode locations on the headset and the active circuit box.

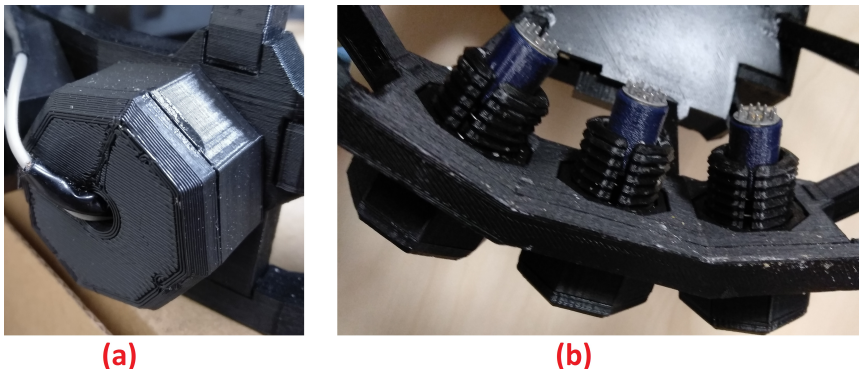

Figure 2.28: (a) The small box containing the active circuit PCB (b) The three spring load dry electrodes mounted on the headset

The headset provides the room for the stimulator PCB and the LEDs array in front of the eyes. It also has the provision to change the the distance of LEDs from the eyes and also the vertical position of the LED array. For normal use the center LED is kept at 15 mm away from the forehead. Figure 2.29 shows the stimulator part of the headset.

The data acquisition hardware and the two DC batteries are also placed on the headset. The complete headset is shown from the tilted left side view in Figure 2.30.

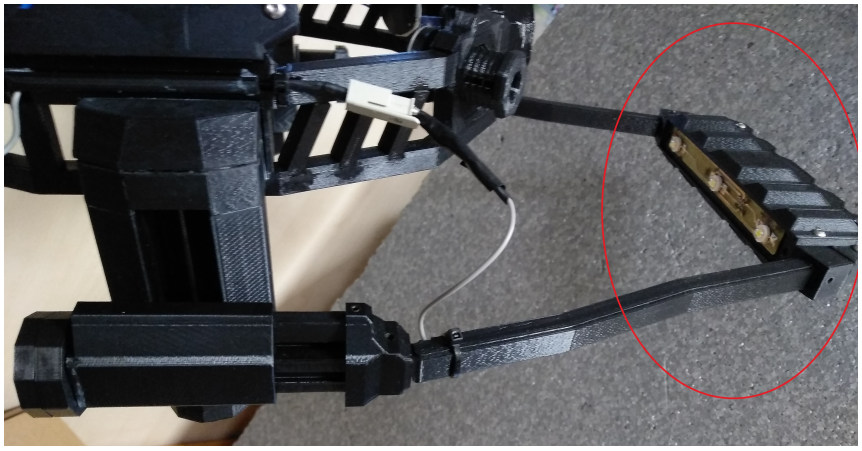

Figure 2.29: The stimulator part of the 3D printed headset (encircled) containing LEDs array and the stimulator circuit PCB

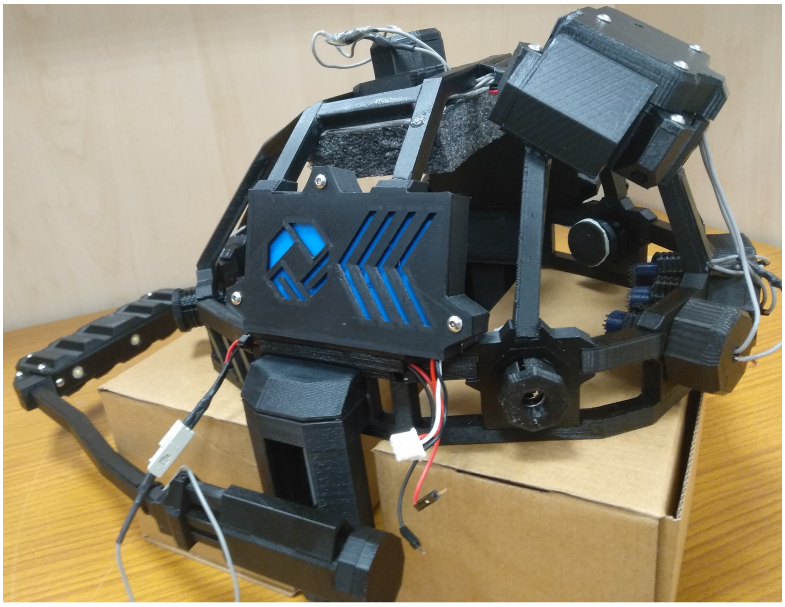

Figure 2.30: The complete 3D printed headset mounting 2 DC batteries, EEG data acquisition hardware, dry active electrodes, and the stimulator

Chapter 3

Experimental Procedures

3.1 Experimental Setup

Before going to perform the experiment on a human subject, a series of preliminary steps are carried out. First of all, it is made sure that following materials/tools required during experiment are available:

a. The BCI system hardware (3D printed headset mounting all the components except DPU and Wifi Rx module)

b. A computer or laptop having MATLAB installed on it (The DPU file "$GUI.m$" should be available in the MATLAB running directory).

c. The wifi Rx module and speakers connected with the computer/Laptop

d. Wet wipes or cotton sticks soaked in alcohol

e. An injection syringe containing the conductive gel (sometimes, gel is needed to apply on the forehead only for better common between the circuit and the body)

f. A toothbrush or any brush having plastic fibers (for cleaning of the electrodes)

g. A volt meter which can measure the DC voltages in the range of $6 - 8.4\ V$

3.1.1 Hardware Setup

The hardware setup includes following steps:

a. First of all make sure that the batteries mounted on the 3D printed headset (called headset from now on) are fully charged. It can be checked by measuring their output voltages. If the output voltage of the battery is greater than $7\ V$, its charging will be sufficient to perform the experiment otherwise charge the battery first.

b. Ask the subject to clean his/her forehead with the wet wipes so that the dead cells on the skin may be cleaned out. Also clean the head skin using alcohol soaked cotton stick by estimating the O1, Oz, O2 and FCz locations of the head using 10-20 international system given in Figure 1.2.

c. Ask the subject to wear the headset so that the electrodes' metallic pins firmly touch the skin on the head as well as forehead skin. You can help him/her in wearing the headset. Adjust the headset using the four supports (two on left and right of the Nasion location, one on the left of O1 position, and one on the right of O2 position) to fix it on the head.

d. Apply the conductive gel between the forehead skin and the nasion electrode

e. Connect both the batteries with the respective circuits by inserting red wire into the connector's red side and black wire into the black side as shown in Figure 3.1.

3.1.2 Software Setup

After completing the hardware setup, perform the following steps on the computer:

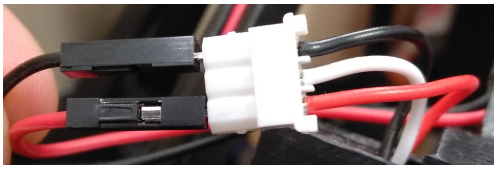

Figure 3.1: The battery connection: red wire male part should be inserted into red side of the battery connector and black wire to the black side

a. First of all, launch the MATLAB software on the computer, open the *GUI.m* file in the MATLAB editor window, and run this file by clicking "run" button in the "Editor" tab or just write "GUI" in the MATLAB command window and hit "Enter". A new popup window will be opened as shown in Figure 3.2.

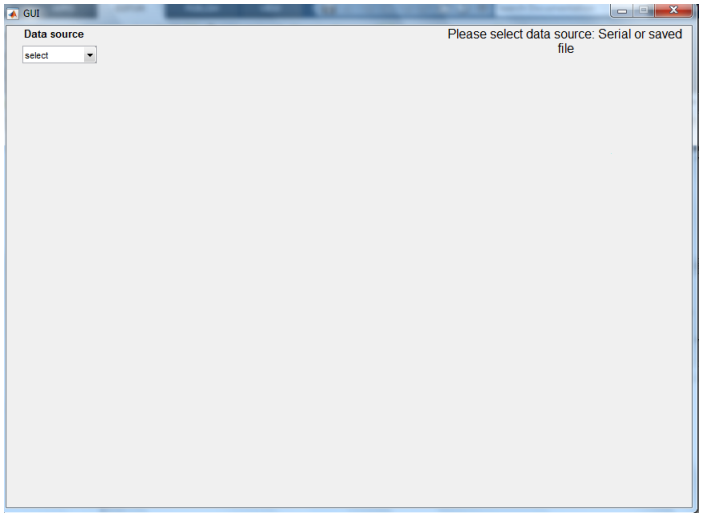

Figure 3.2: Initial GUI window when the "GUI.m" file is run

b. For online experiment on the human subject, select the data source as "Serial" by clicking on the dropdown menu under the heading "datasource" and click "Serial". The GUI window will show the options as shown in Figure 3.3.

c. Fill the fields on the window shown in Figure 3.3. In the "Port" field, input the "COM" port to which the wifi Rx module is connected such as "COM8". Select the EEG channel from the dropdown menu "input channel" and enter the number of recordings, time/recording and sampling rate. You can also

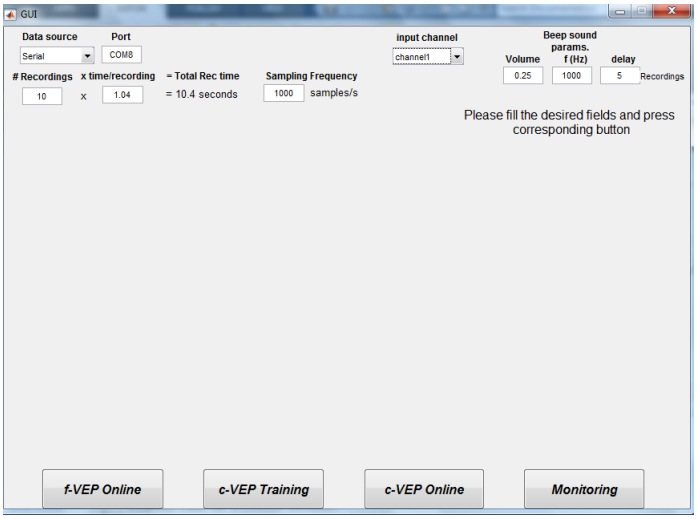

Figure 3.3: GUI window after selecting the datasource (serial for online test or file for offline analysis)

select the volume $(0-1)$ and frequency (pitch) of the beep sound and delay between the two consecutive beeps or leave them to the default values.

3.2 f-VEP Experiment

After performing the setup activities as mentioned in section 3.1, the f-VEP experiments are performed by following some steps as described below:

a. Change the state of the tiny button (located on the stimulator body) to the "OFF" state so that the stimulator starts generating f-VEP signals. The button is shown in the Figure 3.4.

b. Set "no. of recordings" to the desired value and "time/recording" as 1.04.

c. Give the subject instructions about his/her gaze during the experiment. For example, you can ask him to change his/her gaze on every beep if you want to extract the final message string using synchronous method. Otherwise you can set some rule like slow counting in the head.

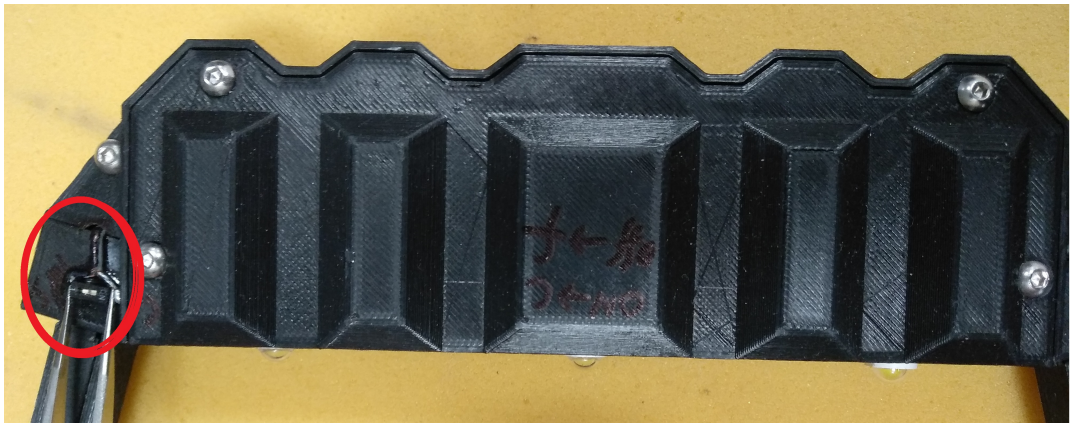

Figure 3.4: The stimulator part of the 3D printed headset: The button to select the stimulation modality (f-VEP or c-VEP) is encircled

d. Press the "f-VEP Online" button on the GUI window and the system will start working. The sample window during the experiment is shown in Figure 3.5.

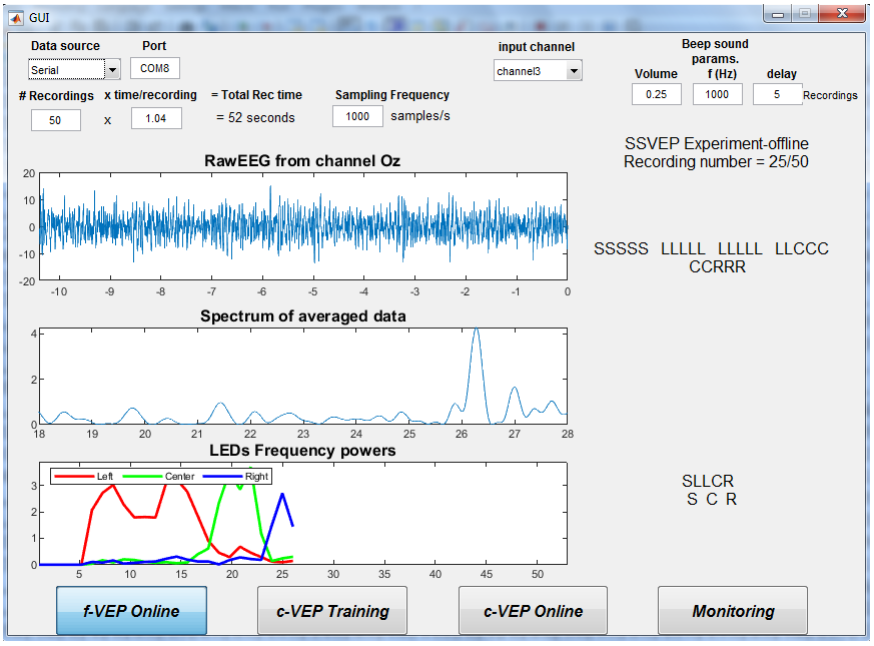

Figure 3.5: A sample GUI window during an online f-VEP experiment

3.3 c-VEP Experiment

In case of performing the c-VEP experiment the following steps are followed:

a. Change the state of the tiny button (located on the stimulator body) to the "OFF" state so that the stimulator starts generating f-VEP signals. The button is shown in the Figure 3.4.

b. Set "number of recordings" as 40 and "time/recording" as 1.05.

c. Ask the subject to focus his/her gaze on the left LED throughout the recording and press the "c-VEP Training" button on the GUI window. It will start the training session for c-VEP.

d. Upon completion of the training session, the template window will be popped up. You can close or minimize this window and come to the main GUI window again and set the "no. of recordings" to any desired number and keep the "time/recording" as 1.05.

e. Give the subject instructions about his/her gaze during the experiment. For example, you can ask him to change his/her gaze on every beep if you want to extract the final message string using synchronous method. Otherwise, you can set some rule like slow counting in the head etc.

f. Press the "c-VEP Online" button on the GUI window and the c-VEP experiment will be started.

3.4 Offline Analysis

The GUI also provides the option to analyze the recorded EEG data in offline mode. The data must be saved in ".txt" file in the form of comma separated bytes as received from the EEG data acquisition hardware. To perform offline analysis, the following steps are performed:

a. Run the GUI.m file as described in section 3.1.2 and select the "datasource" as "File" from as shown in Figure 3.6.

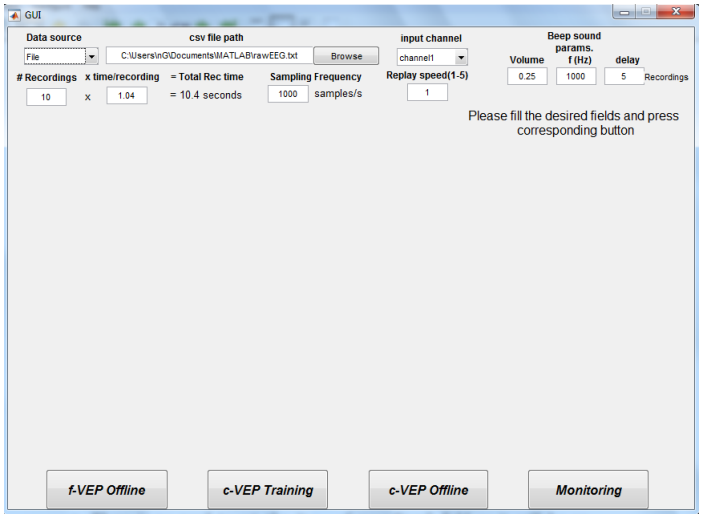

Figure 3.6: The GUI window after selecting the datasource as "File" for offline analysis

b. Input the file path containing the desired file by copying and pasting the path in the "csv file path" or click the browse button and select the desired file from the relevant directory.

c. There is no need to set the "no. of recordings" field as it will be automatically updated by the GUI during offline anlaysis mode. However, "time/recording" can be set by the user.

d. Press the desired button depending upon the type of analysis you want to perform. The options are "f-VEP offline", "c-VEP Training", "c-VEP offline" and "Monitoring". All these options will provide the relevant results in offline mode as if the experiment is being performed online.

Chapter 4

Experimental Results

Experiments are performed on 6 healthy subjects having average age of 31.2 years and standard deviation 5.6 years. The experimental procedures are discussed in detail in chapter 3. The detailed discussion about the results of the experiments is given in the upcoming sections of this chapter.

4.1 Performance Evaluation Metrics

The performance of the BCI systems is normally measured by two common metrics known as "accuracy" and "Information Transfer rate (ITR)". These terms are defined in the following subsections.

4.1.1 Accuracy

By definition, accuracy is calculated as the number of correct target identifications divided by the total number of identifications. It provides the measure how correctly the system is able to detect the target. Percent accuracy is normally reported as percentage of the correct target identifications.

$$\%Accuracy \;=\; \frac{No.\ of\ correct\ target\ identifications}{Total\ no.\ of\ target\ identifications} \;\times\; 100 \qquad (4.1)$$

4.1.2 Information Transfer Rate (ITR)

As clear from the name, it measures the speed of the system (i.e., how much information in terms of bits it can transfer in one minute). The formula to calculate ITR is given in (4.2).

$$ITR\ (bits\ per\ minute) \;= \Big[log(N) + Plog(P) + (1-P)log\frac{1-P}{N-1}\Big] \times \frac{60}{T} \quad (4.2)$$

where

$$N = Number\ of\ targets$$
$$P = Accuracy(0-1)$$
$$T = Time\ required\ to\ identify\ one\ target\ in\ seconds$$

4.2 f-VEP Experiments

4.2.1 Data Collection

As discussed in section 2.4.1, the DPU collects the data as chunks of 12480 bytes in case of f-VEP experiments. This much of data chunk corresponds to 1.04 seconds long recording. This recording time can be changed depending upon the application requirement. The option to change this recording time is provided in the GUI in which it is named as "time/recording" as shown in Figure 3.3.

The data reaches the DPU in the form of "bytes" which is an 8 *bit* data type (0−255 in unsigned format) commonly used in computer programming languages. The DPU saves this data into a "comma separated bytes" format on the hard drive as ".txt" file. The sample data saved is shown in Figure 4.1.

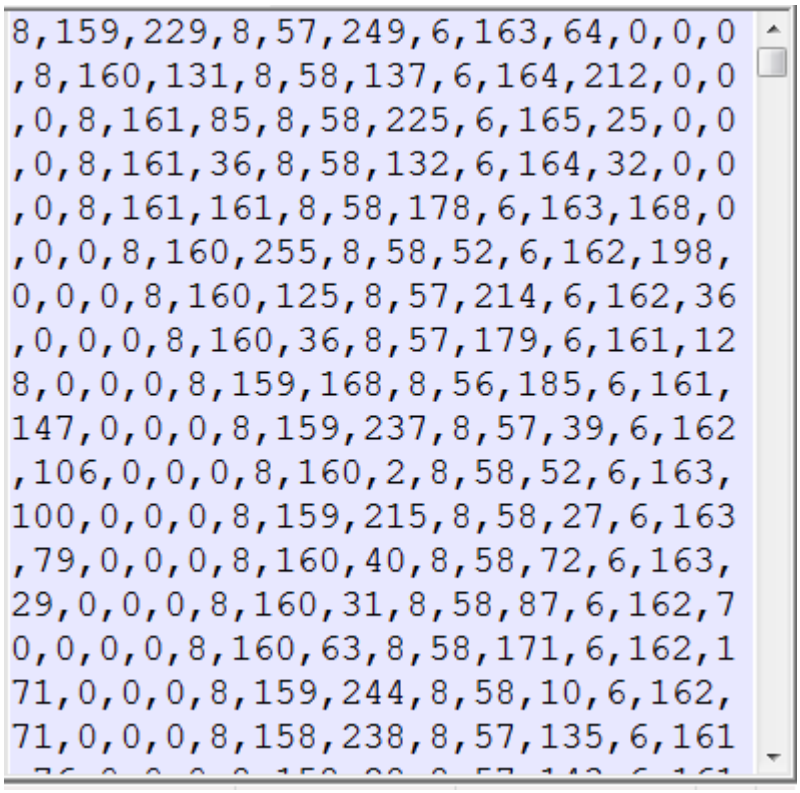

Figure 4.1: A sample raw data shown as comma separated byte values (0-255)

4.2.2 Data Conversion

After receiving the raw data, the DPU converts it into the EEG signal which can be used for further processing. The conversion process is described in detail in section 2.4.2. The raw data is converted into μV level and the signals for each channel are separated from each other. The sample EEG signal extracted for channel "Oz" is shown in Figure 4.2.

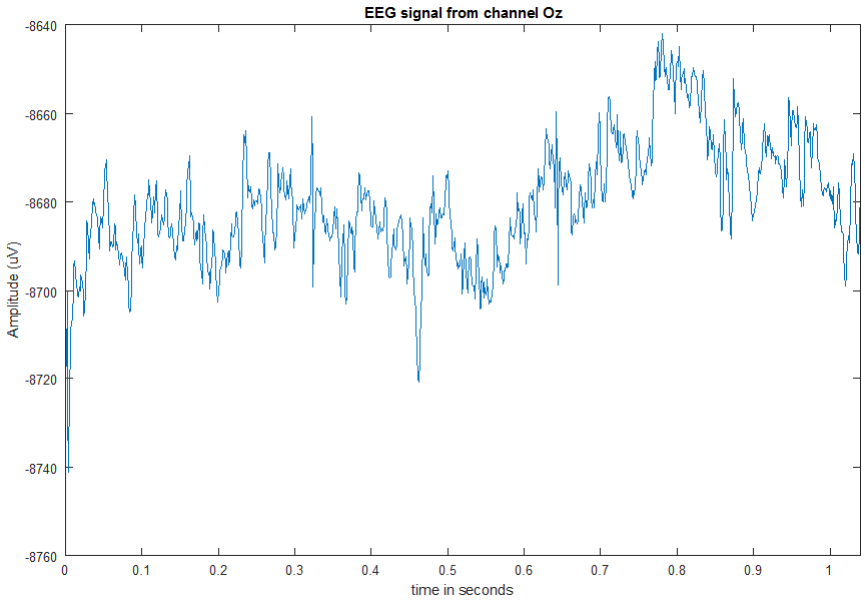

Figure 4.2: A sample raw EEG signal extracted from one f-VEP recording (1.04 seconds) for channel "Oz"

4.2.3 Pre-processing

As can be seen from Figure 4.2, the EEG signal has DC offset and slow variations. Also there are high frequency components in the EEG signal which are of no use with regards to the information. In case of f-VEP response, the EEG signal from the visual cortex has the fundamental frequency of the flickering targets along with their harmonics. In the proposed BCI system 20 Hz, 22.73 Hz, 26.32 Hz are used as the target frequencies and we have considered up to two harmonics. It means that the frequency band of our interest lies between 20 Hz and 78.96 Hz. So, the received EEG signal is passed through a bandpass filter having lower cutoff as 10 Hz and upper cutoff as 90 Hz. A filtered EEG signal and its frequency spectrum is shown in Figure 4.3.

During the recording shown in Figure 4.3, the subject was asked to focus his gaze to the left LED flickering at 20 Hz. The resulting EEG signal has maximum power around 20 Hz, 40 Hz and 60 Hz. So, the resulting EEG signal confirms the claim that the brain responds to the f-VEP stimulus by generating the signal having same fundamental frequency and its harmonics.

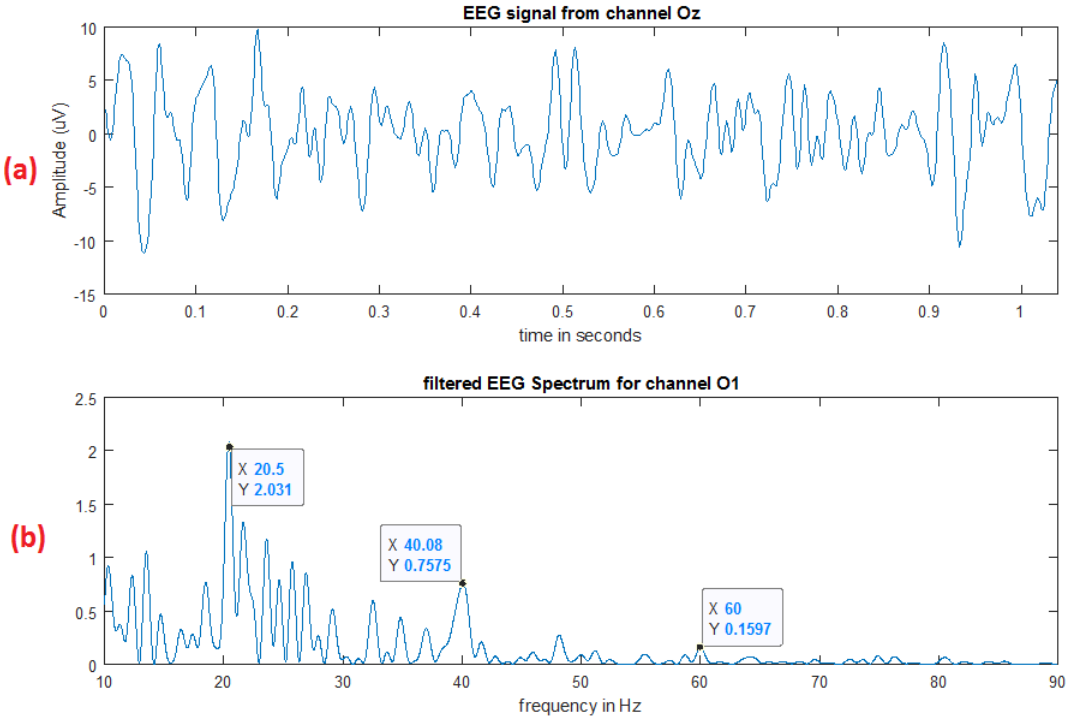

Figure 4.3: (a)The EEG signal after passing through 10-90 Hz bandpass filter and (b) the spectrum of filtered signal

4.2.4 f-VEP Processing

In the proposed BCI system, the newly recorded 1.04 s data is concatenated with the previous two recordings making total of 3.12 s data having 3120 samples. The data is then averaged by using the algorithm explained in section 2.4.3. As a recap, the data is averaged separately for the three frequencies using a sliding window which slides over the 3.12 s data length by using hops equal to the time period of the stimulus waveform. The spectral powers from these three averaged signals are measured by using equation 2.3. The averaged signals and their spectra are shown in Figure 4.4.

According to equation 2.3, the spectral powers shown in figure 4.4 can be calculated as follows:

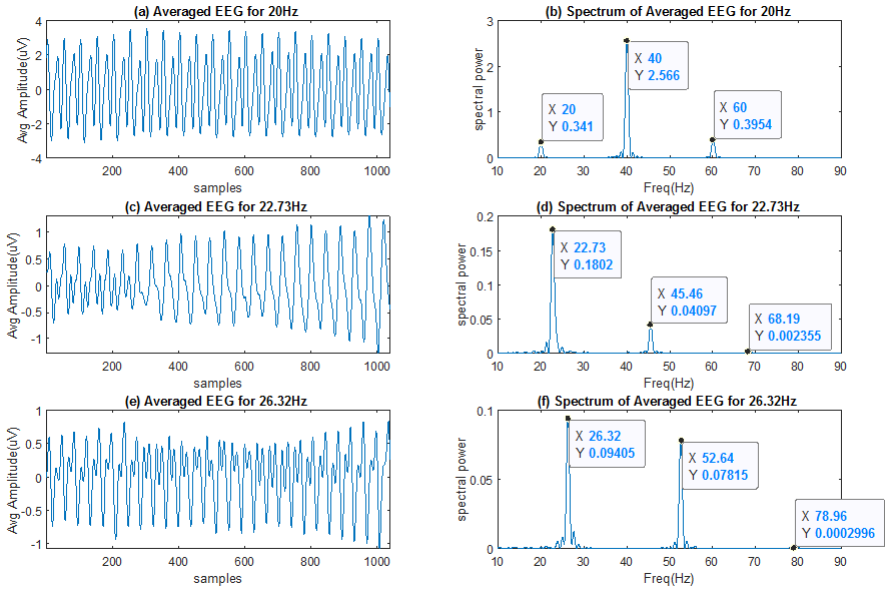

Figure 4.4: The graphs (a),(c),& (e) show the averaged EEG responses corresponding to 20Hz, 22.73Hz, and 26.32Hz respectively and (b),(d),& (f) show their respective spectra

$$\begin{aligned} SP1 &= SP(A1\ in\ [19\ 21], [39\ 41]\ and\ [59\ 61]\ Hz\ bands) \\ &= 0.341 + 2.566 + 0.3954 \\ &= 3.3024 \end{aligned} \tag{4.3}$$

$$\begin{aligned} SP2 &= SP(A2\ in\ [21.73\ 23.73], [44.46\ 46.46]\ and\ [67.19\ 69.19]\ Hz\ bands) \\ &= 0.1802 + 0.041 + 0.002 \\ &= 0.2232 \end{aligned} \tag{4.4}$$

$$\begin{aligned} SP3 &= SP(A3\ in\ [25.32\ 27.32], [51.64\ 53.64]\ and\ [77.96\ 79.96]\ Hz\ bands) \\ &= 0.094 + 0.078 + 0.0002 \\ &= 0.1722 \end{aligned} \tag{4.5}$$

From 4.3, 4.4, and 4.5, the spectral power $SP1$ which corresponds to the averaged EEG response for 20 Hz, is maximum. So, according to the rule defined in Equation 2.4, the DPU will decide that the user was focusing his gaze on the left LED "L" during the time when this EEG data was recorded.

This process is repeated after every recording. On the GUI window, the parameters $SP1$, $SP2$, *and* $SP3$ are plotted on the same graph in real time as red, green, and blue lines respectively. The decisions "L", "C", or "R" are also printed as the string on the GUI window in the space provided under the heading "Live String". Moreover the filtered EEG signal (obtained by current and previous 9 recordings) from the channel used as input for the f-VEP processing is plotted in the top graph of the GUI window. The second graph on the GUI wnidow plots the spectrum of the EEG signal (obtained from current three recordings). All the graphs and strings are updated after one recording time which is set as 1.04 s in our experiments. The sample GUI window after the completion of one experiment is shown in Figure 4.5.

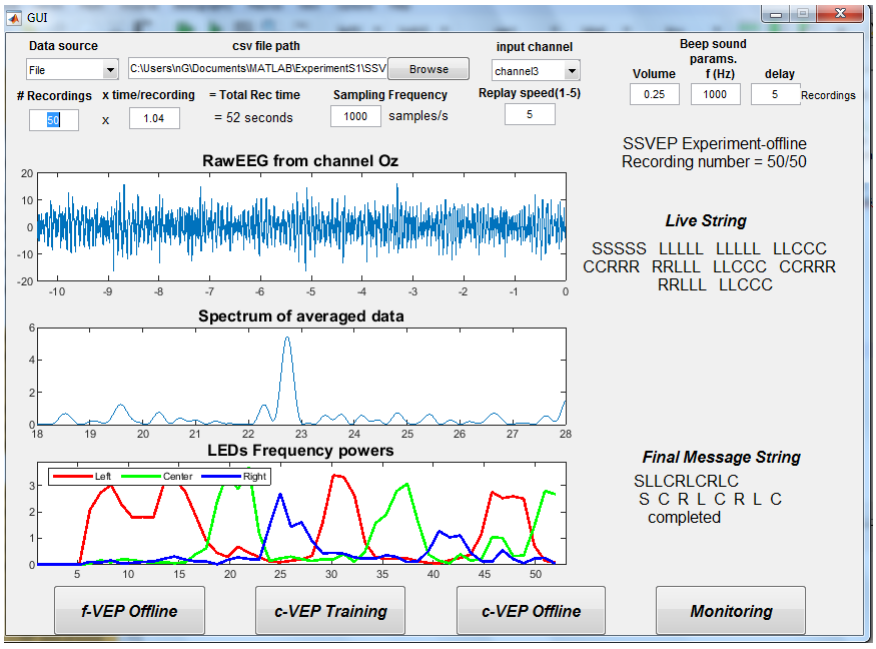

Figure 4.5: A sample GUI window after completing an f-VEP experiment

4.2.5 Results of f-VEP Experiments

As mentioned earlier, the experiments are performed on six healthy subjects. The data is collected from the subjects using sound beeps and synchronous method of final message string extraction as explained in 2.4.5.1. The data is then analyzed in offline mode using asynchronous method (explained in section 2.4.5.2). The GUI provides the offline mode of data analysis in a way as if the experiment is being done in real time.

For the f-VEP experiments, the data is recorded in three or four sessions for each subject depending on the comfortability of the subject. In one of these sessions, the subject was allowed to change his/her gaze according to some sequence of his/her choice. But, these instances of gaze change were synchronized with the beep sounds (separated by $5.2s$ delay) generated by the DPU. For the remaining sessions, the subject was asked to focus the gaze on the same LED (L, C, or R) throughout the recording.

The DPU outputs two types of strings named as "Live string" which is updated after every recording ($1.04\ s$) and "Final Message String" which is updated after every five recordings in synchronous mode or on the instance of gaze change in the asynchronous mode. The algorithm for the extraction of final message string is described in section 2.4.5. The sample view of these strings are shown in Figure 2.25 and 2.26. On the basis of these three outputs (Live string, Final message string in synchronous mode, and final message string in asynchronous mode), three accuracies named as "Live accuracy", "message accuracy" in synchronous mode, and "message accuracy" in asynchronous mode are calculated for each subject. Similarly, three ITR values are calculated using 4.2 named as "Live ITR", "message ITR" for synchronous mode, and "message ITR" for asynchronous mode.

"Live accuracy" is defined as the number of correct decisions in the "Live string" field of the GUI divided by the total number of decisions in live string (updated after every recording of $1.04s$). Similarly, "message accuracy" is defined as the number of correct message characters divided by total number of message

characters. In the same way, "Live ITR" is calculated using the formula given in 4.2 where "P" is taken as the "Live accuracy" and "'T" is taken as $1.04s$. In the calculation of "message ITR" in both the synchronous and asynchronous modes, "P" is taken as the relevant message accuracy and "T" as $5 \times 1.04 \ = \ 5.2s$.

The performance measures of the proposed BCI system implementing f-VEP modality are listed in Table 4.1.

			Synchronous Method		Asynchronous Method	
Subject	Live Accuracy	Live ITR	Message Accuracy	Message ITR	Message Accuracy	Message ITR
	%	bits/min	%	bits/min	%	bits/min
S1	97.8	81.4	100	18.3	100	18.3
S2	98.4	83.9	100	18.3	100	18.3
S3	76.6	32.8	97.4	16	76.4	6.5
S4	81.8	41.5	97.4	16	97.4	16
S5	98.1	85.9	98.1	16.5	100	18.3
S6	100	91.4	100	18.3	100	18.3
Avg* ± std*	92.1 ± 10.2	69.5 ± 25.4	98.8 ± 1.3	17.2 ± 1.2	95.6 ± 9.5	15.9 ± 4.7

Table 4.1: Experimental results showing the proposed BCI system performance in case of f-VEP modality. "Avg" stands for "Average" and "std" stands for "standard deviation".

4.3 c-VEP Experiments

The first two steps i.e. data collection and data conversion are exactly the same as described in sections 4.2.1 and 4.2.2. The only difference is the time/recording which is set as 1.05 s in the c-VEP experiments. The reason behind setting 1.05 s as time/recording is that it contains 1050 samples at the sampling rate of $1000SPS$. So one recording has the EEG response corresponding to exactly 7 runs/trials of the c-VEP code sequence as one sequence takes 150 ms.

4.3.1 Pre-processing

Since the stimulus in case of c-VEP experiments is a pseudo-random code sequence we cannot define the frequency band of our interest. However, we have used a bandpass filter between 4 and 121 Hz to remove the slow variations in the EEG signal due to movements and high frequency components. The raw EEG signal recorded from channel "Oz" before and after filtering is shown in Figure 4.6.

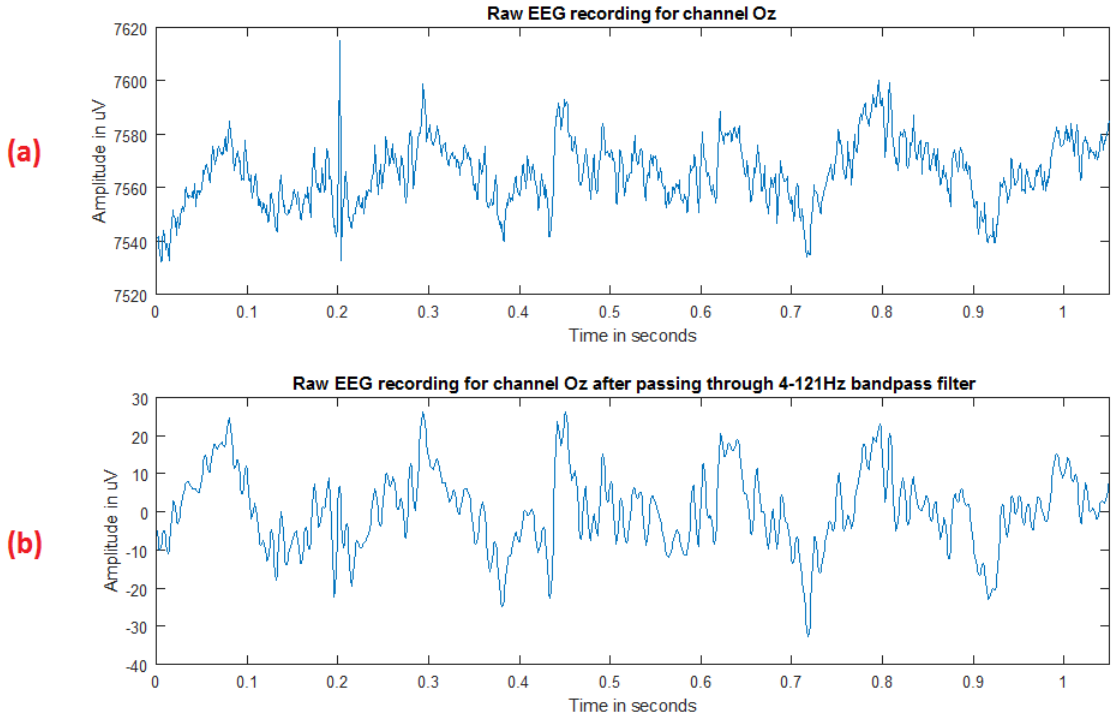

Figure 4.6: (a) One recording (1.05 sec) of raw EEG data for channel Oz (b) The same data after passing through $4 - 121$ Hz bandpass filter

4.3.2 c-VEP Processing

In case of c-VEP experiments, the stimulator generates a marker pulse the onset of which marks the start of each code sequence. These marker pulses are detected at the fourth channel of the received EEG data named as "marker channel". The

onsets of marker pulses are used to separate the EEG responses for each code sequence. The sample data received from channel Oz along with marker pulses is shown in Figure 4.7.

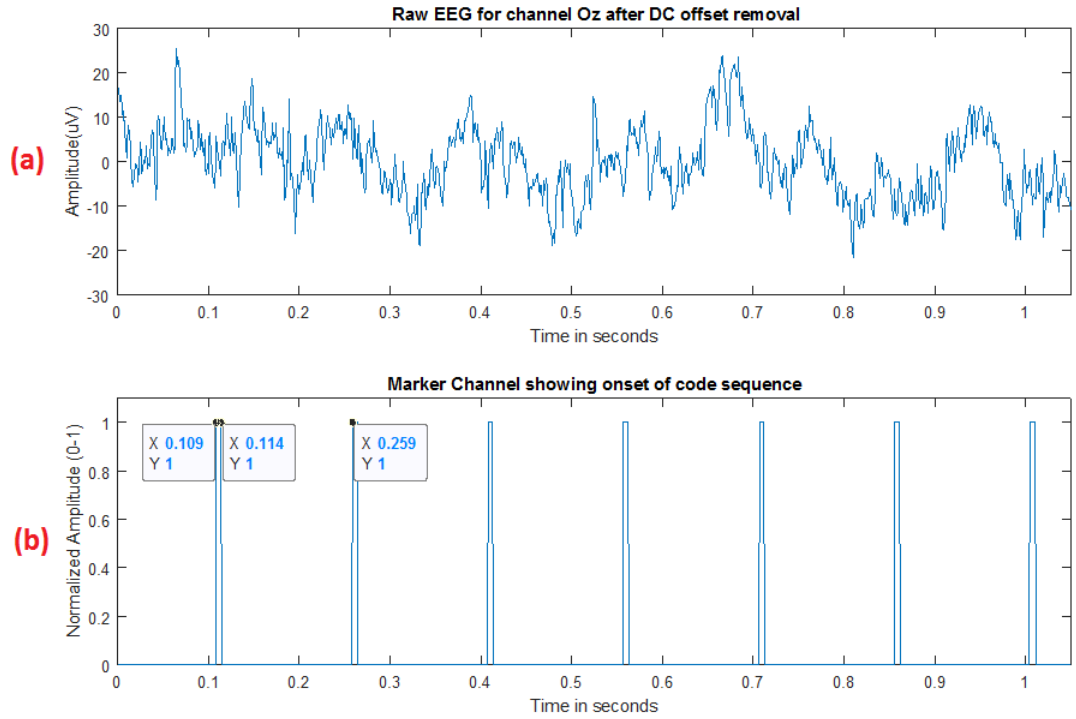

Figure 4.7: (a) One recording of EEG data for channel "Oz" after removal of DC offset (b) The marker channel signal during the same time

In the training session, the subject is asked to focus his/her gaze on the left LED and 40 recordings are done which is equal to the 280 runs/trials of the code sequence as one recording of 1.05 s contains 7 trials. All the EEG responses of the code sequences are separated by taking 150 samples of EEG channels from the onset of the marker pulse. These responses are averaged over number of trials and this averaged response is saved as the target template for Left LED. The templates for other two targets (center and right LEDs) are obtained by circularly shifting the template for left LED by 50 samples (5 $bits$ $\times$ 10 ms/bit) and 100 samples respectively. The template for left LED and corresponding m-sequence are shown in Figure 4.8.

In the test session, the EEG data is collected for 1.05 seconds which contains the EEG response for 7 trials of the c-VEP code. The EEG corresponding to

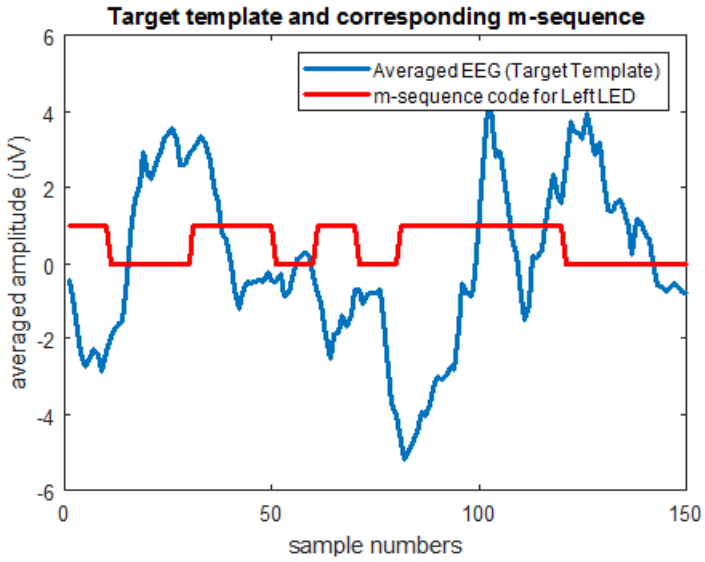

Figure 4.8: The EEG response averaged over the number of trials of the code sequence (blue) and the corresponding code sequence (red)

each run of the code is separated with the help of onset of the marker pulses and averaged over the number of trials. This time the number of averages is much less than that in the training session. This averaged EEG response from one of the channels (say "test signal") is then correlated with the target templates obtained by the training session. The LED (L, C or R) corresponding to the maximum correlation will be selected as the target in real time. The test signal is plotted with the three target templates and the correlations are plotted as bar graph as shown in Figure 4.9

This process is repeated after every recording (1.05 s). On the GUI window, the correlations (say $C1$, $C2$, *and* $C3$) are plotted on the same graph in real time as red, green, and blue lines respectively. The decisions "L", "C", or "R" are also printed as the string on the GUI window in the space provide under the heading "Live String". Moreover, the raw EEG signal (obtained by current and previous 4 recordings) from the channel used as input for the c-VEP processing and the marker channel data for the current recording are shown as separate graphs on the GUI window. All the graphs and strings are updated after one recording time which is set as 1.05 s in our c-VEP experiments. The sample GUI window after completion of one of the experiments is shown in Figure 4.10.

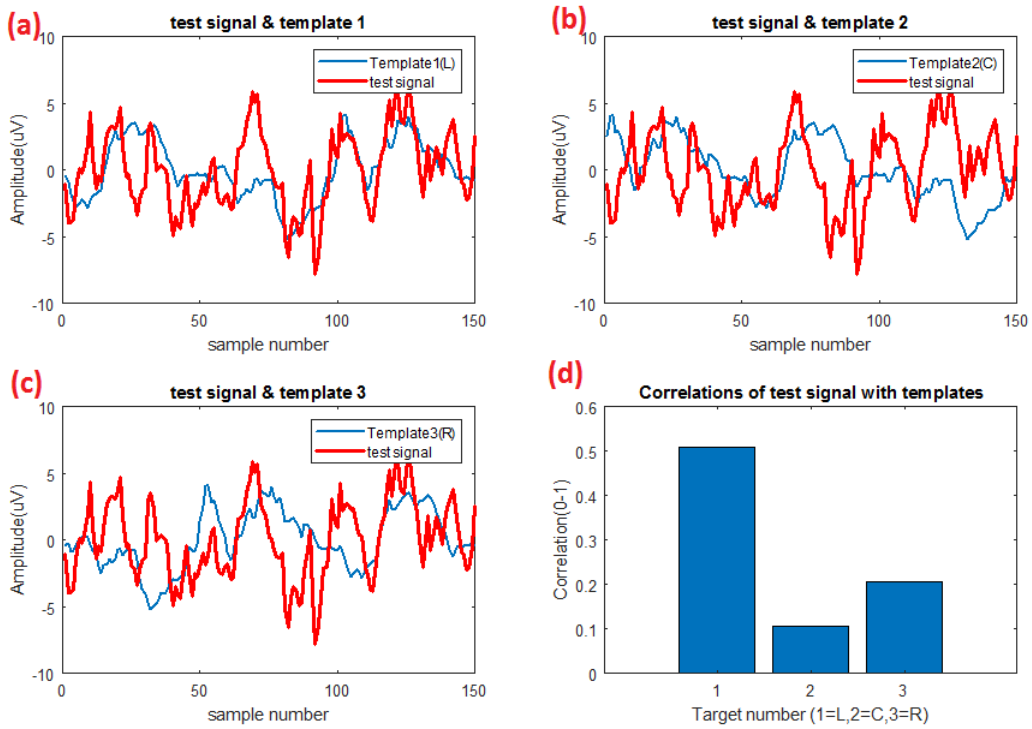

Figure 4.9: (a) The target template1 (blue) and the test signal (red)(b) The target template2 (blue) and the test signal (red)(c) The target template3 (blue) and the test signal (red) (d) The correlations of the test signal with the target templates

4.3.3 Results of c-VEP Experiments

Similar to the f-VEP experiments, the c-VEP experiments are also performed on six healthy subjects. Both the c-VEP and f-VEP experiments are performed on the same subjects in a single sitting. The data is collected from the subjects using sound beeps and synchronous method of final message string extraction as explained in 2.4.5.1. The data is then analyzed in offline mode using asynchronous method (explained in section 2.4.5.2).

The data is recorded in single to four sessions for each subject depending on the comfortability of the subject. In at least one of the sessions, the subject was allowed to change his/her gaze according to some sequence of his/her choice. But, these instances of gaze change were synchronized with the beep sounds (separated by 5.25s delay) generate by the DPU. For the remaining sessions, the subject was

Figure 4.10: A sample GUI window after completion of a c-VEP experiment

asked to focus the gaze on the same LED (L, C, or R) throughout the recording.

The performance parameters "Live accuracy", "message accuracy" in synchronous mode, and "message accuracy" in asynchronous mode are calculated in the similar way as in case of f-VEp experiments. The only difference is the "T" value which is taken as $1.05s$ for calculating "Live ITR" and $5.25s$ for "message ITRs". These performance measures of the proposed BCI system implementing c-VEP modality are listed in Table 4.2.

			Synchronous Method		Asynchronous Method	
Subject	Live Accuracy	Live ITR	Message Accuracy	Message ITR	Message Accuracy	Message ITR
	%	bits/min	%	bits/min	%	bits/min
S1	67	19.5	78.6	7.1	71.4	5
S2	69.1	22.1	93.9	13.7	64.8	3.4
S3	65.7	18.1	85.7	9.7	35.7	0
S4	73.2	27.5	98.6	16.8	61.8	2.8
S5	70.8	24.2	95.8	14.8	78.6	7.1
S6	74.8	29.7	91.7	12.4	74.4	5.8
Avg* ± std*	70.1 ± 3.5	23.5 ± 4.5	90.7 ± 7.4	12.4 ± 3.5	64.5 ± 15.3	4 ± 2.5

Table 4.2: Experimental results showing the proposed BCI system performance in case of c-VEP modality. "Avg" stands for "Average" and "std" stands for "standard deviation".

Chapter 5

Discussion and Conclusion

5.1 Discussion

5.1.1 Cost

Since we aimed at developing a low cost BCI system, we ensured it by using cheap and open source components in the development process. The rough estimates of the component-wise costs are listed in Table 5.1.

No.	Component	Cost estimate (USD)
1	Stimulator	9.345
2	4× active Circuits	3.3
3	EEG data acquisition hardware	65.2
4	Headset (excluding design cost)	215
5	accessories	38.2
Total Cost estimate		331

Table 5.1: The rough estimates of the cost of the prototype BCI system

According to these estimates, the prototype BCI system has been developed in 331 USD. This cost does not include the design cost of the headset which was about 585 USD. The cost can further be reduced for repeated productions as the prices go low when the components are ordered in bulk. Moreover, also the

headset cost can be reduced by using plastic injection moulding technique for bulk productions. The comparison of cost and key features of the commercially available low cost BCI systems is provided in Table 5.2.

Company	Product Name	No. of channels	Sampling rate	Resolution	Functions	Price
			SPS	bits		USD
Open BCI	Low cost biosensing starter kit	4	200	24	EEG monitoring	465
EMOTIV	Insight	5	128	14	measures mental states such as excitement, engagement, relaxation etc.	300
MUSE	muse-2	4	500	Not provided	meditation (Translates brain waves to guiding weather sounds)	150
Neurosky	Mindwave mobile2: brainwave starter kit	1	512	12	EEG monitoring	167
Bilkent University	1^{st} prototype of the proposed BCI system	3	Up to 2000	24	Estimates user's focus on one of the three LED targets	331

Table 5.2: Comparison of cost and key features of the proposed BCI system with commercially available low cost BCI systems

The comparison provided in Table 5.2 shows that the first prototype of the proposed BCI system provides higher sampling rate (up to 2000 SPS) and higher data resolution (24 bit) as compared to the commercially available low cost (< 500 USD) BCI systems.

5.1.2 Wearability

One of the main objective of the thesis is to design and develop a wearable BCI system as mentioned in the section 1.2. This objective is achieved by developing a 3D printed headset which mounts dry electrodes, stimulator, EEG data acquisition hardware, and batteries. The details about the headset are described in section 2.5. At the moment, the first prototype of the proposed BCI system is successfully designed and developed. We will call this first prototype BCI system as "prototype BCI" throughout this chapter.

The prototype BCI is wearable as it can be easily put on or off the subject's head anytime without undergoing prior skin preparation procedures. The problem with the design of first prototype BCI is that it happens to be a little bit uncomfortable for the user if he/she wants to wear it for long time. However, It can be wearable for short times (less than 30 minutes). It becomes uncomfortable because the prototype BCI happens to be a bit heavier in weight. The weight of the headset has the largest contribution to the total weight of the prototype BCI. The headset is heavier than expected due to its solid design and the material used to print it. The solid design means that the square rods on the headset body are solid ones that is to say, they are not like pipes (hollow from inside).

The comfortability and hence the wearability of the prototype BCI system can be improved in two ways:

a. By reducing the weight of the headset: The weight of the headset can be easily reduced by using some light weight material like ABS (Acrylonitrile Butadiene Styrene) and also designing the headset using hollow pipes like structures.

b. The comfortability can be substantially improved by redesigning the dry electrodes. For example, instead of using metal pins to connect with the head skin, some polymer based 3D printed electrodes can be used as suggested in [87], [88], and [89]. The use of polymerized electrodes instead of Ag/AgCl provide much more comfortability and also due to the use of 3D

printing technology, they become much cheaper [87].

5.1.3 Performance

The performance of the prototype BCI system is evaluated using accuracy and ITR metrics as defined in section 4.1. Since the proposed BCI system is an SSVEP based BCI system, its performance evaluation is done using two most common modalities (f-VEP and c-VEP defined in section 1.1.4). The experimental procedures and results obtained are described in detail in chapter 3 and chapter 4, respectively. The performance of the prototype BCI for f-VEP and c-VEP modalities is discussed separately in the following paragraphs.

5.1.3.1 f-VEP Performance

As described in section 4.2.5, the performance of the prototype BCI is evaluated by calculating three types of accuracies and three types of ITRs.

As in Table 4.1, the prototype BCI system has achieved the "Live accuracy" value of $92.1 \pm 10.2\%$ and "Live ITR" as 69.5 ± 25.4 bits/minute. These values are quite satisfactory but looking at their standard deviations, they seem to have large variation among their samples. Looking at individual subject results, the "Live accuracy" and "Live ITR" are quite low for subjects S3 and S4. One of the reason may be the higher noise level in the EEG recordings. The other reasons may be the lack of attention or some unwanted habitual movements during the experiment causing artifacts in the EEG recordings.

Since high variations observed in the "Live accuracy" and "Live ITR" measures, the system generates a final message string on the basis of multiple live decisions obviously to obtain stable results. This is evident from the "message accuracy" and "message ITR" in synchronous method. Using synchronous method of final message extraction, the message accuracy turns out to be $98.8 \pm 1.3\%$ and the message ITR as 17.2 ± 1.2 bits per minute. In case of asynchronous method,

the message accuracy becomes $95.6 \pm 9.5\%$ and message ITR as 15.9 ± 4.7 bits per minute. So, the synchronous method gives better and statistically stable results. The asynchronous method could not improve the stability of the results as it is sensitive to the variations in the samples. The asynchronous method can be improved by applying some error correction techniques in the live string samples. For instance, if there is a different decision character sandwiched in two similar ones such as "RCR", the middle "C" can be replaced by R in the live string. In this way, the number of variations in the live string will be reduced and the message accuracy using asynchronous method will be improved.

As a summary, the prototype BCI performs very well in case of using f-VEP modality and gives high values of accuracies and ITRs.

5.1.3.2 c-VEP Performance

The performance of the prototype BCI is also evaluated using c-VEP modality and the performance metrics are presented in Table 4.2. The system exhibits 70.1% as "Live accuracy" and 23.5 bits per minute as"Live ITR" which are quite low. The major reason of relatively low performance is the use of single channel for c-VEP modality and the quality of the signal. People like Başaklar et al. ([58]) implemented c-VEP modality using multiple channels and employing spatial filtering to improve the SNR (signal to noise ratio) of the EEG signals. The prototype BCI also has three EEG channels for data acquisition, but unfortunately it does not give good quality signal on all the channels simultaneously. The reason is that all the three electrodes do not touch firmly to the skin due to the design flaw in the headset.

The system gives "message accuracy" of 90.72% and "message ITR" of 12.4 bits per minute using synchronous method. The asynchronous method could not improve the message accuracy as it is already sensitive to the variations in live string. Hence, the metrics on the basis of final message are quite satisfactory using c-VEP modality even for single channel.

5.1.3.3 Overall Performance

From sections 5.1.3.1 and 5.1.3.2, it can be safely claimed that the prototype BCI exhibits high values of accuracy on the basis of its final message output using synchronous method in both the f-VEP and c-VEP modalities. All this performance is exhibited using only one EEG channel which means that the system can be further simplified by redesigning its hardware to single channel and hence further reducing the cost and improving the wearability.

5.2 Conclusion

The first prototype of the proposed BCI system is successfully designed and developed. The key features of the prototype BCI system are:

a. It is a low cost system which can be produced by a cost estimate of about 331 US$.

b. It is wearanble. In other words, the user can easily put it on and off without other's help.

c. It is a wireless BCI system using wifi communication to avoid long wires between the computer and the user

d. It is able to distinguish among the three LED targets placed 5 *cm* away from each other and 15 *cm* away from the forehead.

e. It provides higher sampling rates (up to 2000 samples per second) making it able to implement advanced BCI paradigms like c-VEP etc.

f. It provides a simple human machine interface in the form of GUI showing real time EEG signals, live decisions, and final message. The user can select different parameters like input channel, sampling rate, no. of recordings, and time of each recording.

g. It saves the raw data on the disk and provides the option to replay the experiment in offline mode.

h. It provides the clues to the user in the form of short beep sounds so that he/she can synchronize the gaze changes with the sound beeps. The user can select the frequency and volume of the beep sound and also the delay between two consecutive beeps.

The prototype BCI is tested using f-VEP and c-VEP modalities and experiments are performed on six different subjects. The system exhibits high accuracy and good ITR values for both the modalities. For f-VEP modality, it exhibits an average accuracy (live accuracy) of 92.1% and average ITR (live ITR) of 69.5 bits/min on the basis of target identifications done on 1.04 s data recordings. If we extract one message character from five consecutive target identifications, the average accuracy (message accuracy) goes to 98.8% and average ITR (message ITR) to 17.2 bits/min. In case of c-VEP modality, it exhibits live accuracy of 70.1 % and live ITR of 23.5 bits/min on the average while message accuracy of 90.7 % and message ITR of 12.4 bit/min on the average.

Bibliography

[1] Y. Lelievre, Y. Washizawa, and T. M. Rutkowski, "Single trial bci classification accuracy improvement for the novel virtual sound movement-based spatial auditory paradigm," in *2013 Asia-Pacific Signal and Information Processing Association Annual Summit and Conference*, pp. 1–6, IEEE, 2013.

[2] W. Wang, A. D. Degenhart, G. P. Sudre, D. A. Pomerleau, and E. C. Tyler-Kabara, "Decoding semantic information from human electrocorticographic (ecog) signals," in *2011 Annual International Conference of the IEEE Engineering in Medicine and Biology Society*, pp. 6294–6298, IEEE, 2011.

[3] J. S. Brumberg, A. Nieto-Castanon, P. R. Kennedy, and F. H. Guenther, "Brain–computer interfaces for speech communication," *Speech communication*, vol. 52, no. 4, pp. 367–379, 2010.

[4] G. Schalk, D. J. McFarland, T. Hinterberger, N. Birbaumer, and J. R. Wolpaw, "Bci2000: a general-purpose brain-computer interface (bci) system," *IEEE Transactions on biomedical engineering*, vol. 51, no. 6, pp. 1034–1043, 2004.

[5] M. Cheng, X. Gao, S. Gao, and D. Xu, "Design and implementation of a brain-computer interface with high transfer rates," *IEEE transactions on biomedical engineering*, vol. 49, no. 10, pp. 1181–1186, 2002.

[6] P. A. Abhang, B. W. Gawali, and S. C. Mehrotra, *Introduction to EEG-and speech-based emotion recognition*. Academic Press, 2016.

[7] S. N. Abdulkader, A. Atia, and M.-S. M. Mostafa, "Brain computer interfacing: Applications and challenges," *Egyptian Informatics Journal*, vol. 16, no. 2, pp. 213–230, 2015.

[8] L. F. Nicolas-Alonso and J. Gomez-Gil, "Brain computer interfaces, a review," *sensors*, vol. 12, no. 2, pp. 1211–1279, 2012.

[9] A. Kübler, B. Kotchoubey, J. Kaiser, J. R. Wolpaw, and N. Birbaumer, "Brain–computer communication: Unlocking the locked in.," *Psychological bulletin*, vol. 127, no. 3, p. 358, 2001.

[10] J. A. Pineda, "The functional significance of mu rhythms: translating ?seeing? and ?hearing? into ?doing?," *Brain research reviews*, vol. 50, no. 1, pp. 57–68, 2005.

[11] A. Black, "The operant conditioning of central nervous system electrical activity," in *Psychology of Learning and Motivation*, vol. 6, pp. 47–95, Elsevier, 1972.

[12] G. Pfurtscheller and C. Neuper, "Motor imagery and direct brain-computer communication," *Proceedings of the IEEE*, vol. 89, no. 7, pp. 1123–1134, 2001.

[13] K.-H. Lee, L. M. Williams, M. Breakspear, and E. Gordon, "Synchronous gamma activity: a review and contribution to an integrative neuroscience model of schizophrenia," *Brain Research Reviews*, vol. 41, no. 1, pp. 57–78, 2003.

[14] P. Brown, S. Salenius, J. C. Rothwell, and R. Hari, "Cortical correlate of the piper rhythm in humans," *Journal of neurophysiology*, vol. 80, no. 6, pp. 2911–2917, 1998.

[15] L. Zhang, W. He, C. He, and P. Wang, "Improving mental task classification by adding high frequency band information," *Journal of medical systems*, vol. 34, no. 1, pp. 51–60, 2010.

[16] W. M. Leach, "Fundamentals of low-noise analog circuit design," *Proceedings of the IEEE*, vol. 82, no. 10, pp. 1515–1538, 1994.

[17] H. H. Jasper, "The ten-twenty electrode system of the international federation," *Electroencephalogr. Clin. Neurophysiol.*, vol. 10, pp. 370–375, 1958.

[18] C. Kabdebon, F. Leroy, H. Simmonet, M. Perrot, J. Dubois, and G. Dehaene-Lambertz, "Anatomical correlations of the international 10–20 sensor placement system in infants," *Neuroimage*, vol. 99, pp. 342–356, 2014.

[19] D. McFarland and J. Wolpaw, "Eeg-based brain–computer interfaces," *current opinion in Biomedical Engineering*, vol. 4, pp. 194–200, 2017.

[20] L. A. Farwell and E. Donchin, "Talking off the top of your head: toward a mental prosthesis utilizing event-related brain potentials," *Electroencephalography and clinical Neurophysiology*, vol. 70, no. 6, pp. 510–523, 1988.

[21] B. Rivet, A. Souloumiac, V. Attina, and G. Gibert, "xdawn algorithm to enhance evoked potentials: application to brain–computer interface," *IEEE Transactions on Biomedical Engineering*, vol. 56, no. 8, pp. 2035–2043, 2009.

[22] A. Rakotomamonjy and V. Guigue, "Bci competition iii: dataset ii-ensemble of svms for bci p300 speller," *IEEE transactions on biomedical engineering*, vol. 55, no. 3, pp. 1147–1154, 2008.

[23] M. Salvaris and F. Sepulveda, "Visual modifications on the p300 speller bci paradigm," *Journal of neural engineering*, vol. 6, no. 4, p. 046011, 2009.

[24] K. Takano, T. Komatsu, N. Hata, Y. Nakajima, and K. Kansaku, "Visual stimuli for the p300 brain–computer interface: a comparison of white/gray and green/blue flicker matrices," *Clinical neurophysiology*, vol. 120, no. 8, pp. 1562–1566, 2009.

[25] S. Ikegami, K. Takano, N. Saeki, and K. Kansaku, "Operation of a p300-based brain–computer interface by individuals with cervical spinal cord injury," *Clinical Neurophysiology*, vol. 122, no. 5, pp. 991–996, 2011.

[26] J. Hill, J. Farquhar, S. Martens, F. Bießmann, and B. Schölkopf, "Effects of stimulus type and of error-correcting code design on bci speller performance," in *Advances in neural information processing systems*, pp. 665–672, 2009.

[27] G. Pfurtscheller and F. L. Da Silva, "Event-related eeg/meg synchronization and desynchronization: basic principles," *Clinical neurophysiology*, vol. 110, no. 11, pp. 1842–1857, 1999.

[28] K. J. Miller, G. Schalk, E. E. Fetz, M. den Nijs, J. G. Ojemann, and R. P. Rao, "Cortical activity during motor execution, motor imagery, and imagery-based online feedback," *Proceedings of the National Academy of Sciences*, vol. 107, no. 9, pp. 4430–4435, 2010.

[29] H. Yuan and B. He, "Brain–computer interfaces using sensorimotor rhythms: current state and future perspectives," *IEEE Transactions on Biomedical Engineering*, vol. 61, no. 5, pp. 1425–1435, 2014.

[30] G. Pfurtscheller, C. Neuper, G. Muller, B. Obermaier, G. Krausz, A. Schlogl, R. Scherer, B. Graimann, C. Keinrath, D. Skliris, *et al.*, "Graz-bci: state of the art and clinical applications," *IEEE Transactions on neural systems and rehabilitation engineering*, vol. 11, no. 2, pp. 1–4, 2003.

[31] B. Blankertz, F. Losch, M. Krauledat, G. Dornhege, G. Curio, and K.-R. Müller, "The berlin brain-computer interface: Accurate performance from first-session in bci-naive subjects," *IEEE transactions on biomedical engineering*, vol. 55, no. 10, pp. 2452–2462, 2008.

[32] J. R. Wolpaw, D. J. McFarland, and T. M. Vaughan, "Brain-computer interface research at the wadsworth center," *IEEE Transactions on Rehabilitation Engineering*, vol. 8, no. 2, pp. 222–226, 2000.

[33] N. Birbaumer, T. Elbert, A. G. Canavan, and B. Rockstroh, "Slow potentials of the cerebral cortex and behavior.," *Physiological reviews*, vol. 70, no. 1, pp. 1–41, 1990.

[34] T. Hinterberger, S. Schmidt, N. Neumann, J. Mellinger, B. Blankertz, G. Curio, and N. Birbaumer, "Brain-computer communication and slow cortical potentials," *IEEE Transactions on Biomedical Engineering*, vol. 51, no. 6, pp. 1011–1018, 2004.

[35] D. Regan, *Human brain electrophysiology: Evoked potentials and evoked magnetic fields in science and medicine*. Elsevier Science Publishing Co., New York, 1988.

[36] Y. Wang, R. Wang, X. Gao, B. Hong, and S. Gao, "A practical vep-based brain-computer interface," *IEEE Transactions on neural systems and rehabilitation engineering*, vol. 14, no. 2, pp. 234–240, 2006.

[37] J. Yin, D. Jiang, and J. Hu, "Design and application of brain-computer interface web browser based on vep," in *2009 International Conference on Future BioMedical Information Engineering (FBIE)*, pp. 77–80, IEEE, 2009.

[38] X. Gao, D. Xu, M. Cheng, and S. Gao, "A bci-based environmental controller for the motion-disabled," *IEEE Transactions on neural systems and rehabilitation engineering*, vol. 11, no. 2, pp. 137–140, 2003.

[39] J. V. Odom, M. Bach, C. Barber, M. Brigell, M. F. Marmor, A. P. Tormene, and G. E. Holder, "Visual evoked potentials standard (2004)," *Documenta ophthalmologica*, vol. 108, no. 2, pp. 115–123, 2004.

[40] W. M. Perlstein, M. A. Cole, M. Larson, K. Kelly, P. Seignourel, and A. Keil, "Steady-state visual evoked potentials reveal frontally-mediated working memory activity in humans," *Neuroscience letters*, vol. 342, no. 3, pp. 191–195, 2003.

[41] M. Gray, A. Kemp, R. Silberstein, and P. Nathan, "Cortical neurophysiology of anticipatory anxiety: an investigation utilizing steady state probe topography (sspt)," *Neuroimage*, vol. 20, no. 2, pp. 975–986, 2003.

[42] N. Galloway, "Human brain electrophysiology: Evoked potentials and evoked magnetic fields in science and medicine," *The British journal of ophthalmology*, vol. 74, no. 4, p. 255, 1990.

[43] G. Bin, X. Gao, Y. Wang, B. Hong, and S. Gao, "Vep-based brain-computer interfaces: time, frequency, and code modulations [research frontier]," *IEEE Computational Intelligence Magazine*, vol. 4, no. 4, pp. 22–26, 2009.

[44] P.-L. Lee, J.-C. Hsieh, C.-H. Wu, K.-K. Shyu, and Y.-T. Wu, "Brain computer interface using flash onset and offset visual evoked potentials," *Clinical Neurophysiology*, vol. 119, no. 3, pp. 605–616, 2008.

[45] Y. Wang, X. Gao, B. Hong, C. Jia, and S. Gao, "Brain-computer interfaces based on visual evoked potentials," *IEEE Engineering in medicine and biology magazine*, vol. 27, no. 5, pp. 64–71, 2008.

[46] Z. Wu, Y. Lai, Y. Xia, D. Wu, and D. Yao, "Stimulator selection in ssvep-based bci," *Medical engineering & physics*, vol. 30, no. 8, pp. 1079–1088, 2008.

[47] R. Abiri, S. Borhani, E. W. Sellers, Y. Jiang, and X. Zhao, "A comprehensive review of eeg-based brain-computer interface paradigms," *Journal of neural engineering*, 2018.

[48] X. Chen, Y. Wang, M. Nakanishi, X. Gao, T.-P. Jung, and S. Gao, "High-speed spelling with a noninvasive brain–computer interface," *Proceedings of the national academy of sciences*, vol. 112, no. 44, pp. E6058–E6067, 2015.

[49] Y.-J. Chen, S.-C. Chen, I. A. Zaeni, C.-M. Wu, A. J. Tickle, and P.-J. Chen, "The ssvep-based bci text input system using entropy encoding algorithm," *Mathematical Problems in Engineering*, vol. 2015, 2015.

[50] M. Bryan, J. Green, M. Chung, L. Chang, R. Scherer, J. Smith, and R. P. Rao, "An adaptive brain-computer interface for humanoid robot control," in *2011 11th IEEE-RAS International Conference on Humanoid Robots*, pp. 199–204, IEEE, 2011.

[51] N.-S. Kwak, K.-R. Müller, and S.-W. Lee, "A lower limb exoskeleton control system based on steady state visual evoked potentials," *Journal of neural engineering*, vol. 12, no. 5, p. 056009, 2015.

[52] G. R. Muller-Putz and G. Pfurtscheller, "Control of an electrical prosthesis with an ssvep-based bci," *IEEE Transactions on Biomedical Engineering*, vol. 55, no. 1, pp. 361–364, 2007.

[53] G. Pfurtscheller, T. Solis-Escalante, R. Ortner, P. Linortner, and G. R. Muller-Putz, "Self-paced operation of an ssvep-based orthosis with and without an imagery-based ?brain switch:? a feasibility study towards a hybrid bci," *IEEE transactions on neural systems and rehabilitation engineering*, vol. 18, no. 4, pp. 409–414, 2010.

[54] J. Chen, D. Zhang, A. K. Engel, Q. Gong, and A. Maye, "Application of a single-flicker online ssvep bci for spatial navigation," *PloS one*, vol. 12, no. 5, p. e0178385, 2017.

[55] A. Furdea, S. Halder, D. Krusienski, D. Bross, F. Nijboer, N. Birbaumer, and A. Kübler, "An auditory oddball (p300) spelling system for brain-computer interfaces," *Psychophysiology*, vol. 46, no. 3, pp. 617–625, 2009.

[56] A. Kübler, A. Furdea, S. Halder, E. M. Hammer, F. Nijboer, and B. Kotchoubey, "A brain–computer interface controlled auditory event-related potential (p300) spelling system for locked-in patients," *Annals of the New York Academy of Sciences*, vol. 1157, no. 1, pp. 90–100, 2009.

[57] X. Chen, Z. Chen, S. Gao, and X. Gao, "A high-itr ssvep-based bci speller," *Brain-Computer Interfaces*, vol. 1, no. 3-4, pp. 181–191, 2014.

[58] T. Başaklar, Y. Tuncel, and Y. Z. Ider, "Effects of high stimulus presentation rate on eeg template characteristics and performance of c-vep based bcis," *Biomedical Physics & Engineering Express*, vol. 5, no. 3, p. 035023, 2019.

[59] E. Yin, Z. Zhou, J. Jiang, F. Chen, Y. Liu, and D. Hu, "A novel hybrid bci speller based on the incorporation of ssvep into the p300 paradigm," *Journal of neural engineering*, vol. 10, no. 2, p. 026012, 2013.

[60] G. Pfurtscheller, G. R. Müller, J. Pfurtscheller, H. J. Gerner, and R. Rupp, "'thought'–control of functional electrical stimulation to restore hand grasp in a patient with tetraplegia," *Neuroscience letters*, vol. 351, no. 1, pp. 33–36, 2003.

[61] F. Cincotti, D. Mattia, F. Aloise, S. Bufalari, G. Schalk, G. Oriolo, A. Cherubini, M. G. Marciani, and F. Babiloni, "Non-invasive brain–computer interface system: towards its application as assistive technology," *Brain research bulletin*, vol. 75, no. 6, pp. 796–803, 2008.

[62] E. Angelakis, S. Stathopoulou, J. L. Frymiare, D. L. Green, J. F. Lubar, and J. Kounios, "Eeg neurofeedback: a brief overview and an example of peak alpha frequency training for cognitive enhancement in the elderly," *The clinical neuropsychologist*, vol. 21, no. 1, pp. 110–129, 2007.

[63] S. Hanslmayr, P. Sauseng, M. Doppelmayr, M. Schabus, and W. Klimesch, "Increasing individual upper alpha power by neurofeedback improves cognitive performance in human subjects," *Applied psychophysiology and biofeedback*, vol. 30, no. 1, pp. 1–10, 2005.

[64] R. Sitaram, S. Lee, S. Ruiz, M. Rana, R. Veit, and N. Birbaumer, "Real-time support vector classification and feedback of multiple emotional brain states," *Neuroimage*, vol. 56, no. 2, pp. 753–765, 2011.

[65] G. Rota, R. Sitaram, R. Veit, M. Erb, N. Weiskopf, G. Dogil, and N. Birbaumer, "Self-regulation of regional cortical activity using real-time fmri: The right inferior frontal gyrus and linguistic processing," *Human brain mapping*, vol. 30, no. 5, pp. 1605–1614, 2009.

[66] R. C. DeCharms, F. Maeda, G. H. Glover, D. Ludlow, J. M. Pauly, D. Soneji, J. D. Gabrieli, and S. C. Mackey, "Control over brain activation and pain learned by using real-time functional mri," *Proceedings of the National Academy of Sciences*, vol. 102, no. 51, pp. 18626–18631, 2005.

[67] U. Strehl, U. Leins, G. Goth, C. Klinger, T. Hinterberger, and N. Birbaumer, "Self-regulation of slow cortical potentials: a new treatment for children with attention-deficit/hyperactivity disorder," *Pediatrics*, vol. 118, no. 5, pp. e1530–e1540, 2006.

[68] J. E. Walker and G. P. Kozlowski, "Neurofeedback treatment of epilepsy," *Child and Adolescent Psychiatric Clinics*, vol. 14, no. 1, pp. 163–176, 2005.

[69] M. B. Sterman and T. Egner, "Foundation and practice of neurofeedback for the treatment of epilepsy," *Applied psychophysiology and biofeedback*, vol. 31, no. 1, p. 21, 2006.

[70] F. Schneider, H. Heimann, R. Mattes, W. Lutzenberger, and N. Birbaumer, "Self-regulation of slow cortical potentials in psychiatric patients: Depression," *Biofeedback and self-regulation*, vol. 17, no. 3, pp. 203–214, 1992.

[71] F. Schneider, B. Rockstroh, H. Heimann, W. Lutzenberger, R. Mattes, T. Elbert, N. Birbaumer, and M. Bartels, "Self-regulation of slow cortical potentials in psychiatric patients: Schizophrenia," *Biofeedback and Self-regulation*, vol. 17, no. 4, pp. 277–292, 1992.

[72] P. Renaud, C. Joyal, S. Stoleru, M. Goyette, N. Weiskopf, and N. Birbaumer, "Real-time functional magnetic imaging?brain–computer interface and virtual reality: promising tools for the treatment of pedophilia," in *Progress in brain research*, vol. 192, pp. 263–272, Elsevier, 2011.

[73] F. Schneider, T. Elbert, H. Heimann, A. Welker, F. Stetter, R. Mattes, N. Birbaumer, and K. Mann, "Self-regulation of slow cortical potentials in psychiatric patients: alcohol dependency," *Biofeedback and self-regulation*, vol. 18, no. 1, pp. 23–32, 1993.

[74] J. R. Millan and J. Mouriño, "Asynchronous bci and local neural classifiers: an overview of the adaptive brain interface project," *IEEE Transactions on Neural Systems and Rehabilitation Engineering*, vol. 11, no. 2, pp. 159–161, 2003.

[75] J. R. Millan, F. Renkens, J. Mourino, and W. Gerstner, "Noninvasive brain-actuated control of a mobile robot by human eeg," *IEEE Transactions on biomedical Engineering*, vol. 51, no. 6, pp. 1026–1033, 2004.

[76] K. Tanaka, K. Matsunaga, and H. O. Wang, "Electroencephalogram-based control of an electric wheelchair," *IEEE transactions on robotics*, vol. 21, no. 4, pp. 762–766, 2005.

[77] B. Rebsamen, E. Burdet, C. Guan, C. L. Teo, Q. Zeng, M. Ang, and C. Laugier, "Controlling a wheelchair using a bci with low information transfer rate," in *2007 IEEE 10th International Conference on Rehabilitation Robotics*, pp. 1003–1008, IEEE, 2007.

[78] Y. Zhang, D. Guo, F. Li, E. Yin, Y. Zhang, P. Li, Q. Zhao, T. Tanaka, D. Yao, and P. Xu, "Correlated component analysis for enhancing the performance of ssvep-based brain-computer interface," *IEEE Transactions on Neural Systems and Rehabilitation Engineering*, vol. 26, no. 5, pp. 948–956, 2018.

[79] M. Wang, R. Li, R. Zhang, G. Li, and D. Zhang, "A wearable ssvep-based bci system for quadcopter control using head-mounted device," *Ieee Access*, vol. 6, pp. 26789–26798, 2018.

[80] B. J. Edelman, J. Meng, N. Gulachek, C. C. Cline, and B. He, "Exploring cognitive flexibility with a noninvasive bci using simultaneous steady-state visual evoked potentials and sensorimotor rhythms," *IEEE Transactions on Neural Systems and Rehabilitation Engineering*, vol. 26, no. 5, pp. 936–947, 2018.

[81] A. Maye, D. Zhang, and A. K. Engel, "Utilizing retinotopic mapping for a multi-target ssvep bci with a single flicker frequency," *IEEE Transactions on Neural Systems and Rehabilitation Engineering*, vol. 25, no. 7, pp. 1026–1036, 2017.

[82] L. Angrisani, P. Arpaia, D. Casinelli, and N. Moccaldi, "A single-channel ssvep-based instrument with off-the-shelf components for trainingless brain-computer interfaces," *IEEE Transactions on Instrumentation and Measurement*, 2018.

[83] J. Xu, R. F. Yazicioglu, B. Grundlehner, P. Harpe, K. A. Makinwa, and C. Van Hoof, "A 160μw 8-channel active electrode system for eeg monitoring," *IEEE Transactions on Biomedical circuits and systems*, vol. 5, no. 6, pp. 555–567, 2011.

[84] S. Nishimura, Y. Tomita, and T. Horiuchi, "Clinical application of an active electrode using an operational amplifier," *IEEE Transactions on Biomedical Engineering*, vol. 39, no. 10, pp. 1096–1099, 1992.

[85] M. Fernandez and R. Pallas-Areny, "A simple active electrode for power line interference reduction in high resolution biopotential measurements," in *Proceedings of 18th Annual International Conference of the IEEE Engineering in Medicine and Biology Society*, vol. 1, pp. 97–98, IEEE, 1997.

[86] T. Degen, S. Torrent, and H. Jackel, "Low-noise two-wired buffer electrodes for bioelectric amplifiers," *IEEE transactions on biomedical engineering*, vol. 54, no. 7, pp. 1328–1332, 2007.

[87] P. Salvo, R. Raedt, E. Carrette, D. Schaubroeck, J. Vanfleteren, and L. Cardon, "A 3d printed dry electrode for ecg/eeg recording," *Sensors and Actuators A: Physical*, vol. 174, pp. 96–102, 2012.

[88] S. Krachunov and A. Casson, "3d printed dry eeg electrodes," *Sensors*, vol. 16, no. 10, p. 1635, 2016.

[89] A. Velcescu, A. Lindley, C. Cursio, S. Krachunov, C. Beach, C. A. Brown, A. K. Jones, and A. J. Casson, "Flexible 3d-printed eeg electrodes," *Sensors*, vol. 19, no. 7, p. 1650, 2019.

Appendix A

Data

The raw EEG data recorded during the performance evaluation experiments on six subjects is saved in a CD attached to this thesis. The data is saved in a folder named as "Experimental data for thesis". The folder contains six ".rar" files. Each file has self explanatory named ".txt" files which can be used for offline analysis mode of the GUI window. For example, if you open "ExperimentS1.rar" file, you will find files named like "SSVEP_memon_C.txt". This file means that it is saved using f-VEP modality while the subject "memon" was looking at center LED throughout the recording.

Appendix B

Code

Since the prototype BCI system has two programmable microcontroller based circuits (stimulator and EEG data acquisition circuit), they are programmed in Arduino-1.8.5 integrated development environment (IDE) using "C" like arduino programming language. For programming the microcontroller of EEG data acquisition circuit, we have used OpenBCI arduino library which is a free resource. The library files are provided in the attached CD with the name of "$OpenBCI\_8.rar$". The codes for stimulator and EEG data acquisition circuit's micrcontrollers are also provided in the attached CD as "$Stimulator\_cVEP\_SSVEP.rar$" and "$OpenBCI\_8bit\_SD\_aw\_30-05-2019-Marker.rar$" files, respectively. The installation of library is much easy. Just unzip the "$OpenBCI\_8.rar$" file, and copy and paste the extracted "$OpenBCI\_8$" folder to the path "C:\Program Files (x86)\arduino-1.8.5\libraries".

The Wifi Tx and Rx modules need programming. They are also programmed using Arduino-1.8.5 IDE and the code files are provided in the attached CD with the named of "$esp\_WiFi\_UART\_Bridge\_UDP\_STAT.rar$" and "$esp\_WiFi\_UART\_Bridge\_UDP\_AP.rar$", respectively.

The Data processing unit (DPU) is implemented in MATLAB using the code "$GUI.m$". This code is provided in the attached CD. The MATLAB code for

generation of m-sequences is also provided as "*mseqSearch.m*" file.

There are 3 types of PCB designs used in the prototype BCI system (i) active circuit PCB (ii) Stimulator PCB and (iii) EEG data acquisition hardware PCB. The gerber files of these PCBs are also provided in the attached CD.

Appendix C

Bill of Materials

4× Active Circuits						
No.	Name	Value	Qty*	Footprint	Reference Designators	cost ($)
1	Capacitor	100 pF	2	Through hole	C1, C2	0.1
2	Capacitor	10 nF	1	Through hole	C3	0.05
3	Resistor	100 ohm	1	Through hole	R3	0.013
4	Resistor	10 k ohm	1	Through hole	R2	0.011
5	Op-Amp	TLC272	1	SOIC8	U1	0.65
Unit cost of active Circuit						0.824
cost of 4× active Circuits						3.3

Table C.1: Bill of materials of the active circuit

Stimulator						
No.	Name	Value	Qty*	Footprint	Reference Designators	cost ($)
1	Capacitor	100 nF	3	1206	C1,C3,C4	0.15
2	Capacitor	330 nF	1	1206	C2	0.05
3	Capacitor	21 pF	2	1206	C5,C6	0.05
4	Diode	DB3X317K0L	1	Mini3-G3-B	D2	0.55
5	Fuse	MF-MSMF030-2	1	1812	F1	0.36
6	Pin Header	1 × 2	2	2.54mm THT	J1,J4	0.026
7	Pin Header	2 × 3	1	2.54mm THT	J2	0.029
8	Female header	2 × 3	1	2.54mm THT		0.04
9	Resistor	1k ohm	1	1206	R1	0.01
10	Resistor	10k ohm	1	1206	R2	0.01
11	Resistor	1M ohm	1	1206	R3	0.01
12	Resistor	150 ohm	3	1206	R4,R5,R6	0.03
13	Resistor	4.7k ohm	1	1206	R7	0.01
14	switch	tactile	1	SMT	S1	0.06
15	switch	DIP	1	SMT	S2	0.6
16	IC	7805	1	TO220	U1	0.6
17	IC	ATMEGA328P-AU	1	TQFP32	U2	3.12
18	Crystal	ABM3-16.000MHz-B2-T	1	HC49	Y1	1.14
19	LEDs	3W power LED	3	SMT		1.5
20	unit cost of PCB manufacturing					1
Unit cost of Stimulator						9.345

Table C.2: Bill of materials of the stimulator

EEG data acquisition hardware						
No.	Name	Value	Qty*	Footprint	Reference Designators	cost ($)
1	Capacitor	0.01 μF	2	1206	C1,C12	0.1
2	Capacitor	2.2 μF	9	1206	C2, C4, C6, C9, C11, C13, C15, C16, C17	0.45
3	Capacitor	1 pF	2	1206	C3, C38	0.1
4	Capacitor	100 μF	2	1206	C5, C29	0.1
5	Capacitor	10 μF	5	1206	C7, C8, C10, C14, C34	0.25
6	Capacitor	0.1 μF	7	1206	C19, C21, C25, C26, C32, C35, C39	0.35
7	Capacitorr	1 μF	7	1206	C18, C20, C24, C27, C28, C30, C31	0.35
8	Capacitorr	9 pF	2	1206	C22, C23	0.1
9	Resistor	1M ohm	2	1206	R1, R4	0.02
10	Resistor	1k ohm	1	1206	R2	0.01
11	Resistor	4.7k ohm	1	1206	R3	0.01
12	LED	SML-LX23USBC-TR	1	2-SMD	CR1	0.4
13	Fuse	MF-MSMF030-2	1	1812	F1	0.36
14	Diode	DB3X317K0L	3	Mini3-G3-B	U9, U10, U11	1.65
15	Resistor array	CAY16-2201F4LF	3	1206	B3, B5, B8	0.045
16	Capacitor array	CKCL44X7R1H102M085AA	3	0805	C33, C36, C37	0.24
17	ESD protection chip	TPD4E1B06 DCKR	4	SOT-363	B4, B6, B7, B9	2.32

EEG data acquisition hardware						
18	Level shifter	SN74LVCC3245 ADWR	1	24-SOIC	U8	1.36
19	-2.5V regulator	TPS72325DBVR	1	SOT-753	U3	2.8
20	2.5V regulator	TLV70025DDCR	1	SOT-23-5	U4	0.48
21	Voltage inverter	LM2664M6	1	SOT-23-6	U2	0.89
22	5V regulator	LP2989IM-5.0	1	8-SOIC	U1	2.84
23	3.3V regulator	LP5907MFX-3.3	2	SOT-753	U5, U6	1.1
24	Microcontroller	ATMEGA328P-AU	1	TQFP32	B2	3.12
25	EEG chip	ADS1299-4	1	TQFP64	U7	34
26	Crystal	ABM3-16.000MHz-B2-T	1	HC49	Y1	1.14
27	Wifi Tx module	ESP8266	1			3
28	Wifi Rx module	Node microcontroller	1			5.1
29	unit cost of PCB manufacturing					2.5
Unit cost of EEG data acquisition hardware						65.2

Table C.5: Bill of materials of the EEG data acquisition hardware

Headset and accessories		
No.	Name	cost ($)
1	5m single core shielded cable	1
2	Headset design	585
3	Headset printing	215
4	2× 7.4V LiPO batteries (GSP065078)	37.2
Cost of accessories		38.2
Cost of headset		215

Table C.6: Headset and accessories